

AD A 052069

AMRL-TR-77-71



BIOMECHANICAL AND PERFORMANCE RESPONSE OF MAN IN SIX DIFFERENT DIRECTIONAL AXIS VIBRATION ENVIRONMENTS

WILLIAM H. LEVISON

BOLT BERANEK AND NEWMAN, INC.
50 MOULTON STREET
CAMBRIDGE, MASSACHUSETTS 02138

CARIOLD B. HARRAH

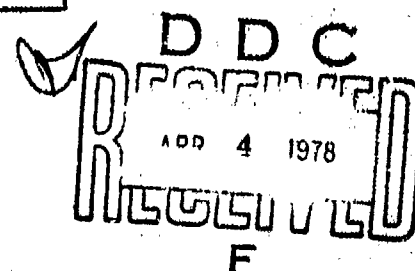
AEROSPACE MEDICAL RESEARCH LABORATORY

SEPTEMBER 1977

TECHNICAL REPORT AMRL-TR-77-71

Approved for public release; distribution unlimited.

AEROSPACE MEDICAL RESEARCH LABORATORY
AEROSPACE MEDICAL DIVISION
AIR FORCE SYSTEMS COMMAND
WRIGHT-PATTERSON AIR FORCE BASE, OHIO



NOTICES

When US Government drawings, specifications, or other data are used for any purpose other than a definitely related Government procurement operation, the Government thereby incurs no responsibility nor any obligation whatsoever, and the fact that the Government may have formulated, furnished, or in any way supplied the said drawings, specifications, or other data, is not to be regarded by implication or otherwise, as in any manner licensing the holder or any other person or corporation, or conveying any rights or permission to manufacture, use, or sell any patented invention that may in any way be related thereto.

Please do not request copies of this report from Aerospace Medical Research Laboratory. Additional copies may be purchased from:

National Technical Information Service
5285 Port Royal Road
Springfield, Virginia 22161

Federal Government agencies and their contractors registered with Defense Documentation Center should direct requests for copies of this report to:

Defense Documentation Center
Cameron Station
Alexandria, Virginia 22314

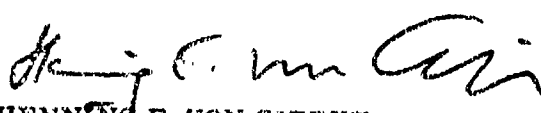
TECHNICAL REVIEW AND APPROVAL

AMRL-TR-77-71

This report has been reviewed by the Information Office (OI) and is releasable to the National Technical Information Service (NTIS). At NTIS, it will be available to the general public, including foreign nations.

This technical report has been reviewed and is approved for publication.

FOR THE COMMANDER


HENNING E. VON GIERKE
Director
Biodynamics and Bionics Division
Aerospace Medical Research Laboratory

REPORT DOCUMENTATION PAGE		READ INSTRUCTIONS BEFORE COMPLETING FORM	
1. REPORT NUMBER	2. GOVT ACCESSION NO.	3. RECIPIENT'S CATALOG NUMBER	
11 AMRL-TR-77-71			
4. TITLE (and Subtitle)	5. TYPE OF REPORT & PERIOD COVERED		
BIOMECHANICAL AND PERFORMANCE RESPONSE OF MAN IN SIX DIFFERENT DIRECTIONAL AXIS VIBRATION ENVIRONMENTS.	BN-3343		
7. AUTHOR(s)	6. PERFORMING ORG. REPORT NUMBER		
William H. Levison/(BBN, Inc.) Carlold B. Harrah/(AMRL)	BBN, Inc. Rpt No. 3343		
	8. CONTRACT OR GRANT NUMBER(s)		
	In part under F33615-76-C-5015		
9. PERFORMING ORGANIZATION NAME AND ADDRESS	10. PROGRAM ELEMENT, PROJECT, TASK AREA & WORK UNIT NUMBERS		
Bolt Beranek and Newman, Inc. 50 Moulton Street Cambridge, Massachusetts 02138	62202F, 7231-01-77		
11. CONTROLLING OFFICE NAME AND ADDRESS	12. REPORT DATE		
Aerospace Medical Research Laboratory, Aerospace Medical Division, Air Force Systems Command, Wright-Patterson Air Force Base, Ohio 45433	11/Sept. 1977		
14. MONITORING AGENCY NAME & ADDRESS (if different from Controlling Office)	13. NUMBER OF PAGES		
	13 91 p.		
	15. SECURITY CLASS. (of this report)		
	UNCLASSIFIED		
	15a. DECLASSIFICATION/DOWNGRADING SCHEDULE		
16. DISTRIBUTION STATEMENT (of this Report)			
Approved for public release; distribution unlimited.			
17. DISTRIBUTION STATEMENT (of the abstract entered in Block 20, if different from Report)			
18. SUPPLEMENTARY NOTES			
19. KEY WORDS (Continue on reverse side if necessary and identify by block number)			
Behavioral and Social Sciences: Man-Machine Biological and Medical Sciences: Stress Physiology Manual Control Human Dynamic Response Vibration Biodynamic Stress Tracking Tasks			
20. ABSTRACT (Continue on reverse side if necessary and identify by block number)			
A series of experiments was performed to explore biodynamic response and tracking performance in various whole-body vibration environments. The primary experimental variable was the direction of the vibration: X+pitch, Y+roll, Z, roll, pitch, and yaw. Tracking axis (pitch or roll) and control-stick spring constant were additional experimental variables. Data from these experiments were analyzed to derive engineering descriptions of biodynamic response and tracking behavior, and a model was developed to relate tracking performance to biodynamic response parameters.			

SECURITY CLASSIFICATION OF THIS PAGE (When Data Entered)

060 100

PREFACE

The experiments described in this report were conducted at the Vibration Branch of the Aerospace Medical Research Laboratory. Major C. B. Harrah was the technical monitor for this contract and project engineer for the AMRL experimental program, and he contributed substantially to the description of experiments in Section 2 of this report. Data analysis and performance modeling were performed by Bolt Beranek and Newman Inc.

ACQUISITION FOR	
NIIS	Whole Section <input checked="" type="checkbox"/>
DDC	5 Section <input type="checkbox"/>
UNANNOUNCED	<input type="checkbox"/>
JUSTIFICATION	
BY	
DISTRIBUTION AVAILABILITY CODES	
Dis	SECRET
A	

TABLE OF CONTENTS

<u>Section</u>	<u>Page</u>
1. INTRODUCTION.	1
2. DESCRIPTION OF EXPERIMENT	4
2.1 Overview	4
2.2 Tracking Task Implementation	4
2.3 Vibration Environment.	6
2.4 Experimental Plan and Data Collection.	10
2.5 Analysis Procedures.	10
3. EXPERIMENTAL RESULTS.	17
3.1 Biodynamic Response.	17
3.2 Tracking Behavior.	35
3.3 Model Analysis	52
4. SUMMARY AND RECOMMENDATIONS	67
APPENDIX - Supplementary Data	71
REFERENCES.	82

LIST OF FIGURES

<u>Figure</u>	<u>Page</u>
1. Tracking Task.	5
2. Procedure for Computing Transfers Related to Y-Axis Platform Vibration.	16
3. Rms Shoulder Acceleration.	18
4. Effect of Stick Configuration on Rms Shoulder Acceleration	22
5. Feedthrough Impedances for Translational Platform Vibration, Pitch Tracking Task	24
6. Feedthrough Impedances for Y-Axis Platform Vibration.	26
7. Feedthrough Impedances for X, Pitch, and Yaw Platform Vibrations, Pitch Tracking Task	27
8. Feedthrough Impedances for Y and Roll Platform Vibrations, Roll Tracking Task	28
9. Feedthrough Impedances for Z-axis Vibration from Three Study Programs	31
10. Feedthrough Impedances for Two Subjects, Z-Axis Platform Vibration, Pitch Tracking Task.	33
11. Shoulder/Platform Describing Functions for Translational Platform Vibration	35
12. Shoulder/Platform Describing Functions for Rotational Platform Vibration.	36
13. Shoulder/Platform Describing Functions for X-Axis Platform Vibration.	38
14. Shoulder/Platform Describing Functions for Y-Axis Platform Vibration.	39
15. Shoulder/Platform Describing Functions for Z-Axis Platform Vibration.	40
16. Effect of Vibration on Rms Tracking Performance Scores, Pitch Task	41

LIST OF FIGURES (Cont'd.)

<u>Figure</u>		<u>Page</u>
17.	Effect of Vibration on Rms Tracking Performance Scores, Roll-Task.	42
18.	Relation Between Rms Tracking Error and Rms Shoulder Acceleration.	46
19.	Effect of Longitudinal-Axis Platform Vibration on Pilot Frequency Response, Pitch Task.	47
20.	Effect of Lateral-Axis Platform Vibration on Pilot Frequency Response, Pitch Tracking Task.	48
21.	Effect of Lateral-Axis Platform Vibration on Pilot Frequency Response, Roll Tracking Task	49
22.	Ratios of Rms Performance in a Z-Axis Vibration Environment to Rms Performance in a Static Environment.	51
23.	Diagram of the Model Structure	54
24.	Linear Flow Diagram of the Tracking Task	59
25.	Comparison of Predicted and Measured Rms Performance Scores for Five Experimental Conditions	61
26.	Comparison of Predicted and Measured Rms Performance Scores for Three Study Programs	63
27.	Comparison of Predicted and Measured Frequency Response	64

LIST OF TABLES

<u>Table</u>	<u>Page</u>
1. Control Stick Parameters.	7
2. Platform Acceleration Parameters.	9
3. Experimental Conditions	11
4. Presentation of Experimental Conditions	12
5. Tape Channel Identification	13
6. Results of T-Tests on Rms Acceleration Scores	20
7. Comparison of Experimental Parameters for Three Studies	32
8. Results of T-Tests of Tracking Scores	44
A1. Average Rms Biodynamic Response Acceleration.	71
A2. Average Control/Platform Describing Functions	72
A3. Impedance Model for Stick Feedthrough	73
A4. Average Shoulder-X/Platform Describing Functions.	74
A5. Average Shoulder-Y/Platform Describing Functions.	75
A6. Average Shoulder-Z/Platform Describing Functions.	76
A7. Average Elbow/Platform Describing Functions	77
A8. Average Rms Tracking Scores	78
A9. Average Frequency-Response Measures, Stiff Stick.	79
A10. Average Frequency-Response Measures, Spring Stick	79
A11. Significance of Vibration/Static Differences in Frequency Response, Stiff Stick.	80
A12. Significance of Vibration/Static Differences in Frequency Response, Spring Stick	80
A13. Significance of Pitch-Task/Roll-Task Differences in Frequency Response	81

1. INTRODUCTION

This report summarizes a joint effort by the Aerospace Medical Research Laboratory (AMRL) and Bolt Beranek and Newman Inc. (BBN) to explore biomechanical response and tracking performance in various vibration environments. This effort was conducted as part of the long-range AMRL study program to obtain performance data and develop models for human performance in vibration environments. Recent studies pertinent to this program have explored the nature of biomechanical response and the interactions between tracking, vibration, and control-stick parameters [1-4].

The study reported here had two primary objectives: (1) to obtain basic biomechanical response and tracking performance data for whole-body vibration applied individually or in combination along the six translational and rotational axes, and (2) to implement a computerized model (to operate on a CDC-6600 digital computer) that is capable of predicting biodynamic response and tracking performance in various vibration environments. This report reviews the results of the experimental study and consequent model development; details of the computer model are given in a companion document [5].

Recent AMRL/BBN study programs, exploring Z-axis vibration inputs only, have yielded the following conclusions:

1. Shoulder and head response to platform vibration is independent of control-stick parameters, whereas the portion of control response linearly correlated with the vibration input ("stick feedthrough") depends strongly on stick parameters.

2. Stick location has no significant effect on rms tracking error score or on biomechanical response.
3. Stick feedthrough can be represented analytically by an impedance model that includes the stick impedance plus two impedance functions, independent of stick design, that account for biodynamic response behavior.
4. Biomechanical response mechanisms are essentially linear for the range of vibration amplitudes and spectra explored in these studies.
5. Vibration degrades tracking performance largely by interfering with basic pilot information-processing capabilities; stick feedthrough typically has a secondary effect. Visual effects appear to have been of minor consequence. In terms of the pilot/vehicle model used in these studies, the important effects appear to be an increase in motor related sources of randomness in the pilot's response plus an increase in the pilot's time delay. A recent study [4] indicated that motor noise/signal ratio and time delay increased linearly with rms shoulder acceleration.

The results of this study extend the results of earlier studies by providing data relevant to vibration along axes other than the Z-axis. Previous conclusions are only partially confirmed. The effects of vibration on tracking performance are again largely represented by changes in model parameters related to pilot randomness and time delay. The relationship between

these parameters and biodynamic response found in the previous study must be modified, however, to provide a consistent explanation of tracking performance. Specifically, if time delay and motor noise variance are allowed to vary linearly with rms shoulder acceleration and inversely with rms control force, tracking data from a number of studies can be accounted for with a single set of independent model parameters. As in previous studies, biodynamic response to Z-axis platform vibration is independent of control-stick design parameters. For other axes of vibration, statistically significant differences in biodynamic response accompany changes in stick parameters.

2. DESCRIPTION OF EXPERIMENT

2.1 Overview

The experimental portion of this investigation was devoted to the experimental design and data collection necessary to provide performance and vibration data suitable for analysis. The objective of the investigation was to determine the effect of rotational and combined-axis vibration on tracking performance. In the test situation, the subject(s) performed a one-dimensional compensatory tracking task while seated on the Sixmode shake table in an upright position. Also located on the vibration table were the control stick and CRT display. The main experimental variable was the direction of vibration input. Both biodynamic and performance responses were investigated.

2.2 Tracking Task Implementation

The single axis tracking task required compensatory tracking to keep a displayed dot centered vertically on a CRT. A simplified schematic of the control loop is shown in Figure 1.

The tracking (e.g., plant disturbance) input consisted of a sum of five sinusoids with component frequencies of .502, 1.256, 3.015, 6.28 and 10.46 rad/sec. The amplitudes were selected to approximate a first-order noise process having a break frequency at 2 rad/sec. This tracking input was summed with the pilot's control input to form a manipulative signal to the plant which is represented by the pot-integrator combination (e.g., $4/s$ dynamics). The plant output, e , was then attenuated so that one volt produced a 0.38 inch displacement of the displayed tracking target (dot) from the center of the CRT (cross-hairs). Both

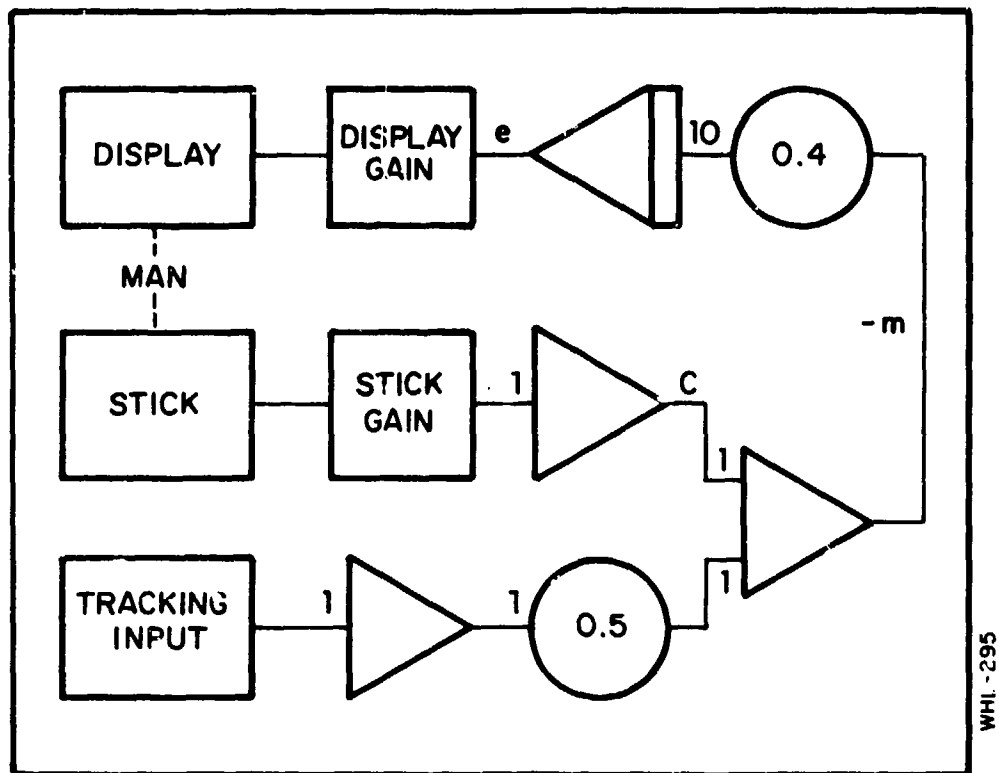


Figure 1. Tracking Task

horizontal "roll" (side-to-side motion of dot) and vertical "pitch" (up-down motion of dot) tracking tasks were employed in different experimental conditions, but the combined task (e.g., two dimensional tracking) was not used. The tracking subject attempted to keep the dot centered by means of a side-mounted control stick. In the horizontal tracking task, right and left motion of the stick produced right and left motion of the dot, respectively. In the vertical tracking task, forward and backward motion of the stick produced downward and upward motion of the dot, respectively. In the experiment, both a "stiff stick" and "spring stick" were used. Table 1 summarizes the control stick parameters.

2.3 Vibration Environment

The vibration environment was supplied by a large amplitude multi-degree of freedom hydraulic vibration table named the Sixmode. It has six degrees of motion including X, Y, Z, roll, pitch and yaw. This table has a payload capacity of 1,000 lbs. and is capable of sinusoidal, sum of sines and random vibration. The experiment used a sum of five sines vibration with equal acceleration at 2, 3.3, 5, 7 and 10 hertz. The rms level of table acceleration was no greater than 0.25g and had a crest factor of 3 giving the subject a maximum peak acceleration of no more than 1g depending on how the sines added together.

The vibration environment was manipulated by changing the direction of application. The six vibration directions used were Z-axis (e.g., vertical for upright, seated subject), roll (R), pitch (P), yaw, X-axis (chest-back) + pitch, and Y-axis (lateral) + roll. With regard to the combined modes of X+pitch and Y+roll, only the linear axis was driven directly. That is, when the

Table 1
Control Stick Parameters

Parameter	Control Stick	
	Stiff	Spring
K_C Electrical gain, volts/pound	0.9	0.333
K_e Electrical gain, volts/inch	117	2.5
K_S Spring gradient, pounds/inch	130	7.0
B_S Stick damping, pounds/(inch/sec)	.0103	.027
M_S Stick mass, pounds	0.7	0.7

shaketable was driven in the X-axis, the pitch motion was produced by cross-coupling between the driving actuators. Similarly, "free" roll was produced when the table was driven in the Y-axis. Because these "free" rotational modes were not directly driven the acceleration spectrums were not as flat (e.g., there was more energy in the 10 Hz region) as the linear mode in the combination.

Average rms platform accelerations measured during the experiments are given in Table 2a. The input was relatively "pure" for Z-axis translational vibration and for the three rotational-axis conditions; that is, vibration power in the nominal axis was clearly dominant over power in the remaining axes. As noted above, X- and Y-axis vibrations were accompanied by a significant amount of rotational-axis vibration.

Table 2b shows that the power spectra for the translational axes were quite flat, as was the spectrum for yaw-axis platform vibration.* Roll and pitch vibration inputs showed resonance behavior in the vicinity of 7 Hz. Because of the Sixmode elastomeric coupler resonances, the Y- and yaw-axis platform vibration also contained substantial power in the vicinity of 14 Hz (not shown in Table 2), even though no electrical input was provided at this frequency to the platform drive system.

Transfer functions relating rotational-axis cross-coupling to primary-axis vibration are shown in Table 2c. Both roll/Y and pitch/X couplings show a sharp increase with frequency. Thus, in the case of nominal X and Y platform vibration, biomechanical response was dominated by the primary translational vibration input at lower frequencies and by the coupled rotational inputs at higher frequencies.

*0 dB = 1 g for translational acceleration, 1 rad/sec² for rotational acceleration.

Table 2
Platform Acceleration Parameters

a) Rms Platform Acceleration*

Vibration Condition	Response Variables					
	X	Y	Z	Roll	Pitch	Yaw
X	0.240	0.005	0.015	0.16	2.3	0.24
Y	0.020	0.21	0.051	1.7	0.23	0.78
Z	0.016	0.022	0.26	0.89	0.51	0.13
Roll	0.005	0.032	0.021	2.5	0.20	0.073
Pitch	0.057	0.007	0.052	0.30	2.6	0.12
Yaw	0.041	0.037	0.011	0.25	0.38	2.1

b) Power in Principal Vibration Axis (dB)

Frequency		Axis of Vibration					
Hz	rad/sec	X	Y	Z	Roll	Pitch	Yaw
2	12.5	-20.2	-23.1	-19.0	0.5	0.8	-2.7
3.3	21	-20.8	-23.6	-19.2	0	-0.4	-4.0
5	31	-20.8	-23.1	-19.6	0.1	1.2	-4.6
7	44	-20.0	-22.5	-19.3	3.5	3.2	-3.6
10	63	-18.2	-25.1	-19.6	-3.8	-3.2	-4.0

c) Relation Between Secondary and Primary Vibration

Frequency		Roll/Y		Pitch/X	
Hz	rad/sec	Gain (dB)	Phase (deg)	Gain (dB)	Phase (deg)
2	12.5	-1.9	-5	-1.1	2
3.3	21	2.2	-10	5.6	-7
5	31	8.9	-9	13.0	-20
7	44	18.8	-18	22.1	-51
10	63	25.3	-147	22.4	-153

*Translational acceleration in g, rotational acceleration in rad/sec².

2.4 Experimental Plan and Data Collection

Twelve members of the hazardous duty panel were used as subjects in the experiment. Prior to the formal sessions, both static and vibration training sessions were used to establish baseline tracking performance for all subjects in all experimental conditions.

Table 3 identifies the nine experimental conditions in terms of the vibration modes and tracking tasks. Including the static run, each condition is characterized by four runs and either the pitch or roll tracking task. Each individual tracking run lasted two minutes. The formal data collection sessions were conducted over a six-day period. Table 4 shows the order in which these experimental conditions were presented to the 12 subjects.

All data was collected on 14-channel magnetic (FM) tape for subsequent analysis. Table 5 lists the four channels of performance data and 10 channels of acceleration data. The only body accelerations measured were at the shoulder and elbow. A triaxial accelerometer was taped to the top of the shoulder and oriented to respond to X, Y, and Z motion, with respect to the conventional body coordinate system. A linear accelerometer was taped to the elbow and aligned to sense lateral arm motion (Y-axis).

2.5 Analysis Procedures

2.5.1 Performance Scores

Standard deviation scores were computed for all important tracking and biodynamic variables. These scores were computed over a 100-second measurement interval that commenced approximately

Table 3
Experimental Conditions

A1	A2	A3
Z X + P P Static "Pitch Task"	P X + P Static Z "Pitch Task"	X + P P Z Static "Pitch Task"
B1	B2	B3
Static R Y + R Yaw "Pitch Task"	Y + R Yaw Static R "Pitch Task"	Y + R Static R Yaw "Pitch Task"
C1	C2	C3
Y + R Yaw Static R "Roll Task"	Static R Y + R Yaw "Roll Task"	Yaw Y + R Static R "Roll Task"

NOTE: The vibration conditions for training runs will consist of (Z, R, P, Yaw, X + P, Y + R) with the pitch task and (R, Yaw, Y + R) with the roll task.

Table 4
Presentation of Experimental Conditions
Day

Subject	5	6	7	8	9	10
1	A1	C2	B1	A2	C1	B2
2	B2	C1	A2	B1	C2	A1
3	C3	B3	A3	C3	B3	A3
4	A3	B1	C3	A1	B3	C1
5	B1	A2	C1	B2	A1	C2
6	C2	A3	B2	C3	A2	B3
7	A3	C1	B3	A1	C3	B1
8	B1	C2	A1	B2	C1	A2
9	C2	B3	A2	C3	B2	A3
10	A3	B1	C3	A1	B3	C1
11	B1	A2	C1	B2	A1	C2
12	C2	A3	B2	C3	A2	B3

Table 5
Tape Channel Identification

<u>Channel</u>	<u>Description</u>
1	Tracking Input(i)
2	Stick Signal(c)
3	Plant Input(m)
4	Error(e)
5	Elbow Y-Acceleration
6	Shoulder Triax, X-Acceleration
7	Shoulder Triax, Y-Acceleration
8	Shoulder Triax, Z-Acceleration
9	Table, Roll-Acceleration
10	Table, Pitch-Acceleration
11	Table, Yaw-Acceleration
12	Table, X-Acceleration
13	Table, Y-Acceleration
14	Table, Z-Acceleration

15 seconds after initiation of the experimental trial. As all variables had essentially zero mean, we shall use the term "rms performance score" in the remainder of this report to signify the standard deviation score.

T-tests were performed on paired difference scores to determine the statistical significance of experimental factors on performance.

2.5.2 Frequency-Response Measures

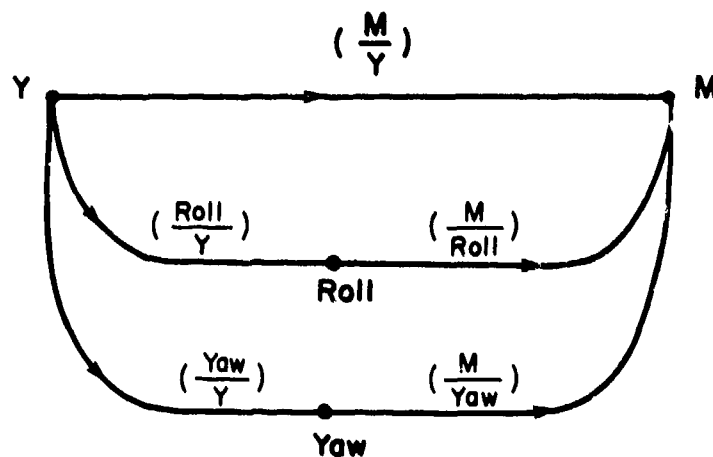
Power spectra were computed using fast-Fourier transform techniques. Spectra were computed from data covering a 100-second measurement interval coincident with the interval used in computing rms performance scores. Spectra were separated into input-correlated and remnant-related components using the techniques employed in the previous study [4].

Pilot and biodynamic describing functions were computed as described previously [4] and were averaged across the experimental subjects for presentation in this report. Pilot describing functions, which showed relatively little variation across subjects, were processed by averaging the amplitude ratios and phase shifts. Biodynamic describing functions, which tended to be more individualistic, were converted to real and imaginary parts for averaging. Average response was then transformed to amplitude ratio and phase shift for presentation.

Because of the rotational-axis vibration input accompanying nominal X- and Y-axis platform vibration, describing functions computed directly from the Fourier transforms had to be "corrected" to determine the describing functions relating to the translational

vibration input alone. The correction scheme for relating some variable "m" (control, shoulder, or elbow) to the Y vibration input is shown in Figure 2. The describing function (M/Y) is the transmissibility relating "m" to the Y-axis input alone. T is the relation between M and Y that is obtained directly from the measurements (which is confounded by the response to the coupled roll and yaw axes). (ROLL/Y) and (YAW/Y) are the transfer functions relating roll and yaw inputs to the nominal Y-axis input and are measured in the same experimental trials as T. The describing functions (M/ROLL) and (M/YAW) must be obtained in experiments in which roll and yaw, respectively, are the only significant vibration inputs. The scheme for computing X-related transmissibility is similar to that shown in Figure 2, except that pitch vibration is the only rotational platform input coupled to the X-axis input.

*The assumption is made that the biodynamic response to roll (or yaw) vibration in the combined-axis vibration environment is the same as the response to roll (or yaw) platform vibration alone. That is, we assume that these response mechanisms are essentially linear and that the various responses are additive in the combined-axis situation. A recent study of biodynamic response to Z-axis vibration suggests that the magnitudes of the body and limb accelerations induced in the subject study were within the linear range of biodynamic response [4].



WHL-374

$$\left(\frac{M}{Y} \right) = T - \left(\frac{\text{Roll}}{Y} \right) \cdot \left(\frac{M}{\text{Roll}} \right) - \left(\frac{\text{Yaw}}{Y} \right) \cdot \left(\frac{M}{\text{Yaw}} \right)$$

T = Describing function relating M to Y obtained directly from measurements

Figure 2. Procedure for Computing Transfers Related to Y-Axis Platform Vibration

3. EXPERIMENTAL RESULTS

Principal experimental results are presented in this section. Except where noted, all results represent average behavior of the experimental subjects. Discussed in order are biodynamic response, tracking behavior, and model analysis. Supplemental data are contained in the Appendix.

3.1 Biodynamic Response

3.1.1 Rms Acceleration Scores

Rms shoulder accelerations for the three translational response axes, along with total rms shoulder acceleration*, are shown in Figure 3 for the six vibration conditions. Data are given for the pitch tracking task and have been averaged across stiff-stick and spring-stick conditions. Rms scores for shoulder and elbow response are tabulated separately for the two stick configurations and for the two axes of tracking in Table A1 of the Appendix.

The magnitude of the shoulder response was considerably different for the various vibration inputs. The response to X+pitch vibration was over three times as great as the response to Y+roll vibration (total response), with the response to Z vibration roughly midway between the two. The differential effects of rotational vibration inputs were even greater, with the response to pitch inputs about six times as great as the response to yaw.

*Total rms response was computed as the square root of the sum of the mean squared response scores in the X, Y, and Z axes.

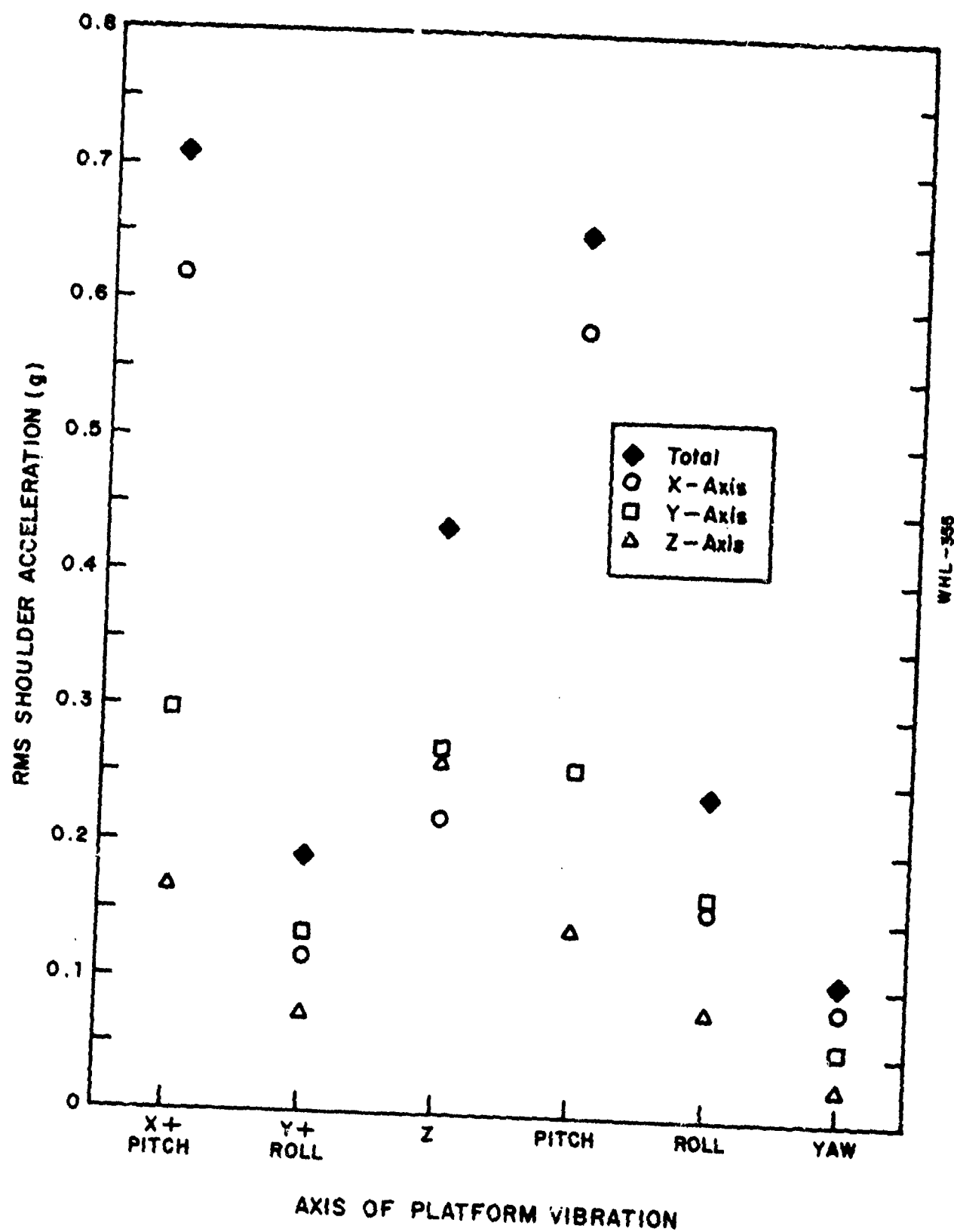


Figure 3. Rms Shoulder Acceleration

The X+pitch, pitch, and yaw vibration conditions induced shoulder motion largely in the axis of expected response (i.e., the X shoulder axis for these three vibration inputs, as well as Y-axis response to yaw inputs). Considerable cross-coupling was evident in the remaining vibration conditions. Y-, Z-, and roll-axis platform vibration all induced a sizeable X-axis shoulder response. In addition, the Y-directed response dominated when the platform was vibrated in the Z-axis.

In general, the degree of correlation between platform vibration and shoulder response appears to be in the axes of direct coupling. For example, the fractions of response power correlated with the Z-axis vibration input were 0.55, 0.57, and 0.39 for the X-, Y-, and Z-axis response measurements. Biodynamic describing functions (shown later in this section) support this hypothesis.

Although the data shown in Figure 3 have been averaged across stick configurations for convenience, stick configuration significantly influenced rms shoulder acceleration. Table 6 shows that stick configuration had a significant* effect on shoulder response in about one-third of the response situations. That is, if we consider the four response variables shown in Table 6, the six vibration conditions, and the two axes of tracking, there are a total of 36 situations in which we can explore the effects of stick configuration on biodynamic response (the combined entries of Tables 6a and 6b). In 13 of these situations, the rms average acceleration score measured when the

*Differences significant at the 0.05 significance level or lower are considered "significant".

Table 6

Results of T-Tests on Rms Acceleration Scores

Vibration Condition	<u>Significance Level</u>			Elbow
	Shoulder-X	Shoulder-Y	Shoulder-Z	

a) Effect of Stick Configuration, Pitch Task

X	.05	.05	-	-
Y	-	.001	.05	.05
Z	-	-	-	-
Roll	-	.01	-	-
Pitch	.01	.05	-	-
Yaw	-	.05	.05	-

b) Effect of Stick Configuration, Roll Task

Y	-	-	.01	-
Roll	-	-	-	-
Yaw	.05	-	.01	-

c) Effect of Tracking Axis, Stiff Stick

Y	-	.01	-	-
Roll	-	-	-	-
Yaw	-	-	-	-

d) Effect of Tracking Axis, Spring Stick

Y	-	.01	-	.01
Roll	-	-	-	-
Yaw	-	-	-	-

subjects tracked with the stiff differed significantly from the corresponding score obtained when tracking was done with the spring stick. In only 3 out of 24 cases (combined entries of Table 6c and 6d) was the rms acceleration score significantly dependent on whether pitch or roll was tracked.

Y-axis and total rms shoulder acceleration are shown for the two stick configurations for the pitch tracking task in Figure 4. Accelerations were greater for the stiff stick for all but the Z-axis vibration condition. Accelerations were slightly greater for the spring stick configuration in the Z-axis case but, as found in previous studies [3, 4], these differences were not statistically significant. Apparently, for vibration inputs not along the Z-axis, the mechanical loading of the stick is an important component of the overall biodynamic response system.

3.1.2 Stick Feedthrough

Describing functions relating control input to platform vibration were transformed to yield the following impedance model for stick feedthrough:

$$C_v = \frac{ZT}{ZO+ZS} \cdot K_e \cdot \alpha_p \quad (1)$$

where C_v = response of control stick to platform vibration due to direct biomechanical coupling (volts)

α_p = platform acceleration (g)

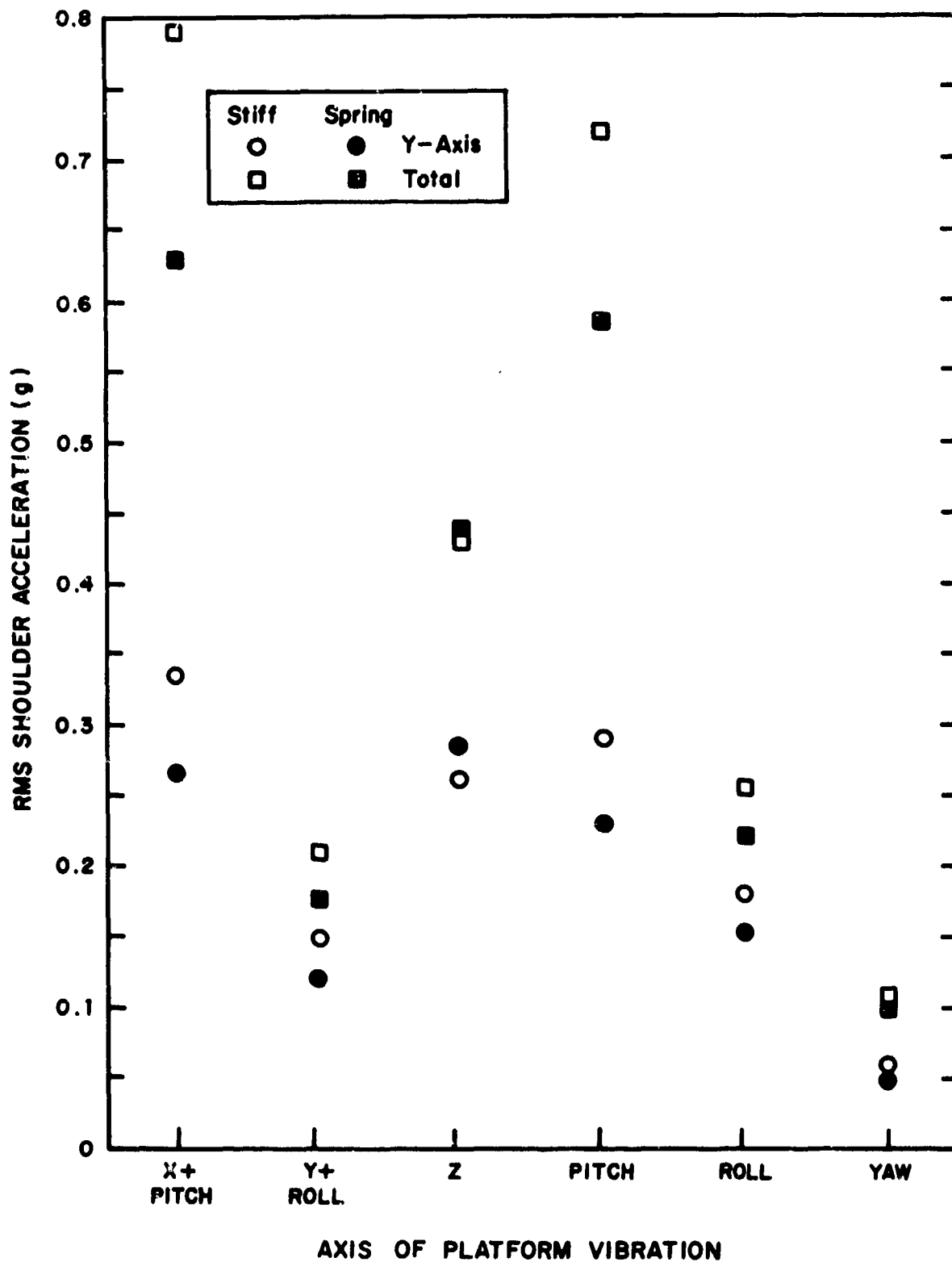
K_e = control gain (volts/inch)

ZT = feedthrough transfer impedance (pounds/g)

ZO = feedthrough output impedance (pounds/inch)

ZS = stick impedance (pounds/inch)

This model is a frequency-domain representation; the argument ($j\omega$) has been omitted for notational convenience.



WHL - 356

Figure 4. Effect of Stick Configuration on Rms Shoulder Acceleration

Ideally, the impedance functions Z_T and Z_O represent biomechanical properties of the man and the man/platform interface that are independent of control-stick parameters. Z_T represents the force that would be imparted to an isometric control task, whereas Z_O represents the ratio of this force to the displacement that would be imparted to a completely free-moving stick. An earlier study of the interaction between control-stick parameters and biomechanical response indicates that this is a workable assumption for Z-axis vibration. In the absence of data either supportive or adverse, we have extended this assumption to other axes of vibration.

Control/platform describing functions are tabulated in Table A2 of the Appendix; impedance parameters derived from these data are given in Table A3. Impedance models for selected experimental conditions are diagrammed in Figures 5 through 10.

Figure 5 shows that impedance functions relating fore-aft control motions to translational platform vibration have similar variations with frequency except that the response to Y-axis vibration exhibits a sizeable peak at the lowest vibration frequency (2 Hz). At remaining vibration frequencies, the strengths of the responses to Y and Z vibrations are nearly equal; the response to X-axis vibration is considerably greater, however. Note that the Y-axis vibration is orthogonal to the direction of control response; thus, the corresponding impedance function represents a form of cross-coupling between vibration input and biodynamic response.

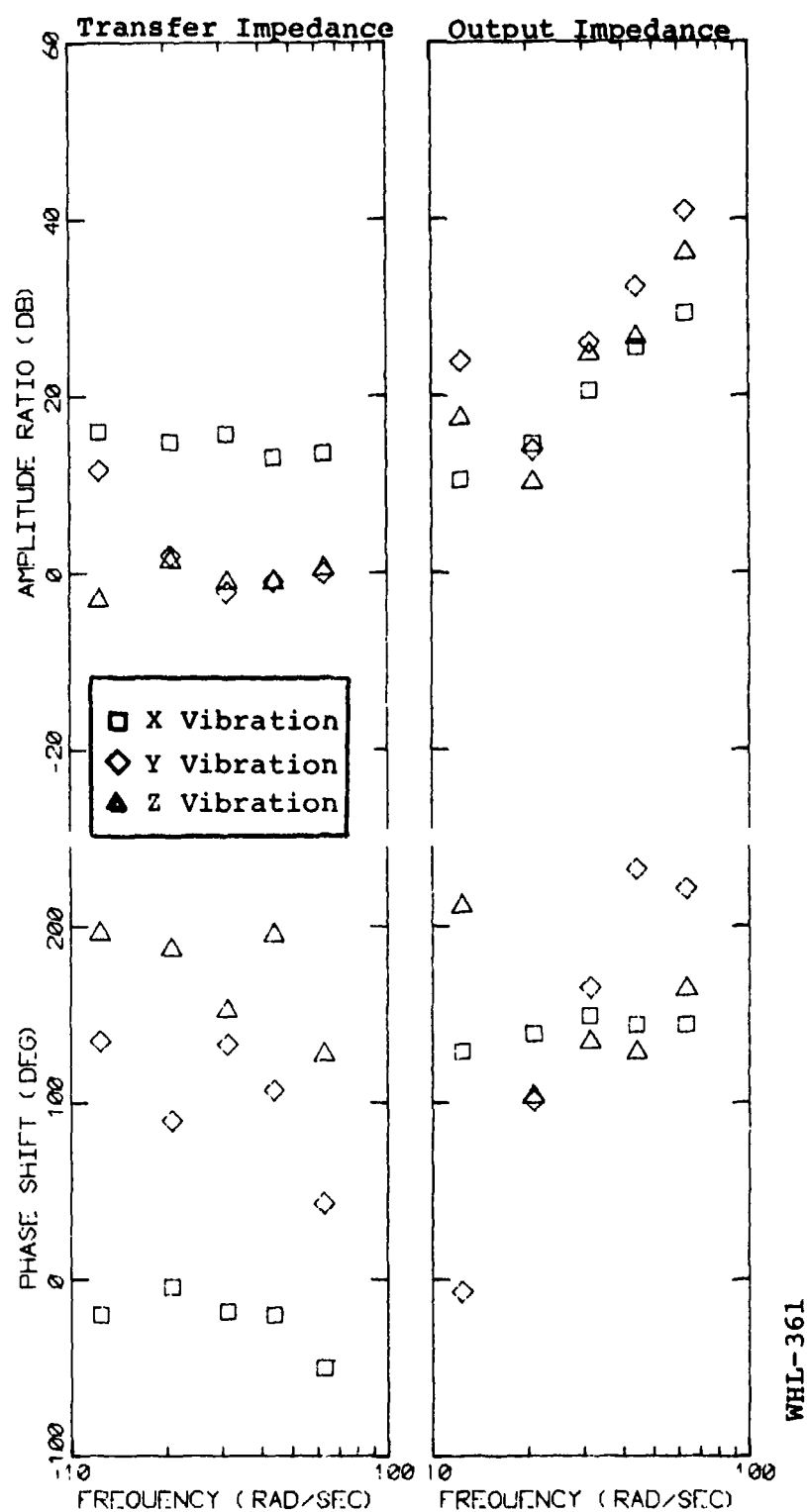


Figure 5. Feedthrough Impedances for Translational Platform Vibration, Pitch Tracking Task

0 dB = 1 pound/g for transfer impedance
 0 dB = 1 pound/inch for output impedance

Figure 6 compares the transfer impedances representing feedthrough from Y-axis platform vibration to fore-aft control response (pitch tracking task) and side-to-side control response (roll tracking task). As expected, the strength of the colinear response path was greater. In addition, the output impedance associated with roll tracking was substantially lower at most measurement frequencies than the impedance associated with pitch tracking.

Figure 7 compares feedthrough impedance functions relating fore-aft control motions to X, pitch, and yaw vibrations - vibration inputs that are expected to couple directly to the response. Frequency dependencies for the three impedance functions are virtually identical; the only important difference is in the overall gain of the transfer impedance. Figure 8 shows a similar relation between impedance functions relating side-to-side control motions to Y and roll vibration inputs.

Comparison of the curves shown in Figure 7 with those of Figure 8 reveal consistent differences in feedthrough impedance functions related to longitudinal-axis vibration and control and lateral-axis vibration and control. The transfer impedances related to longitudinal-axis inputs (Figure 7) are relatively flat with frequency showing a gradual decrease in amplitude ratio with increasing frequency. The lateral-axis transfer impedances shown in Figure 8 show U-shaped ratios, with minimum transfer in the frequency range of 3-5 Hz.

The output impedances differ in the manner observed earlier in Figure 6. The longitudinal-axis impedance increase asymptotically with frequency at about 40 dB per decade, whereas the lateral-axis output impedance seem to asymptote (at least in the measurement range) to an increase with frequency of 20 dB per decade.

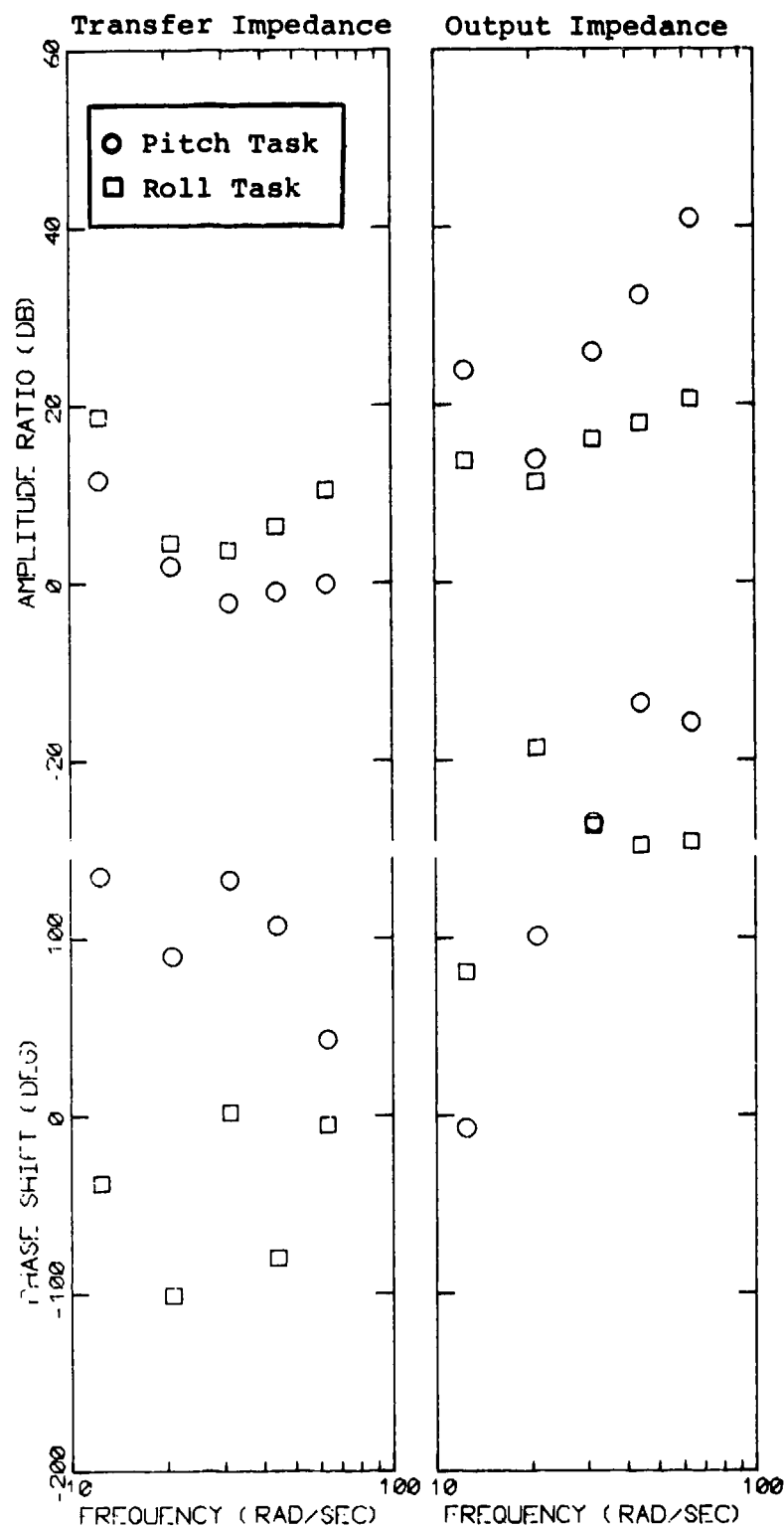
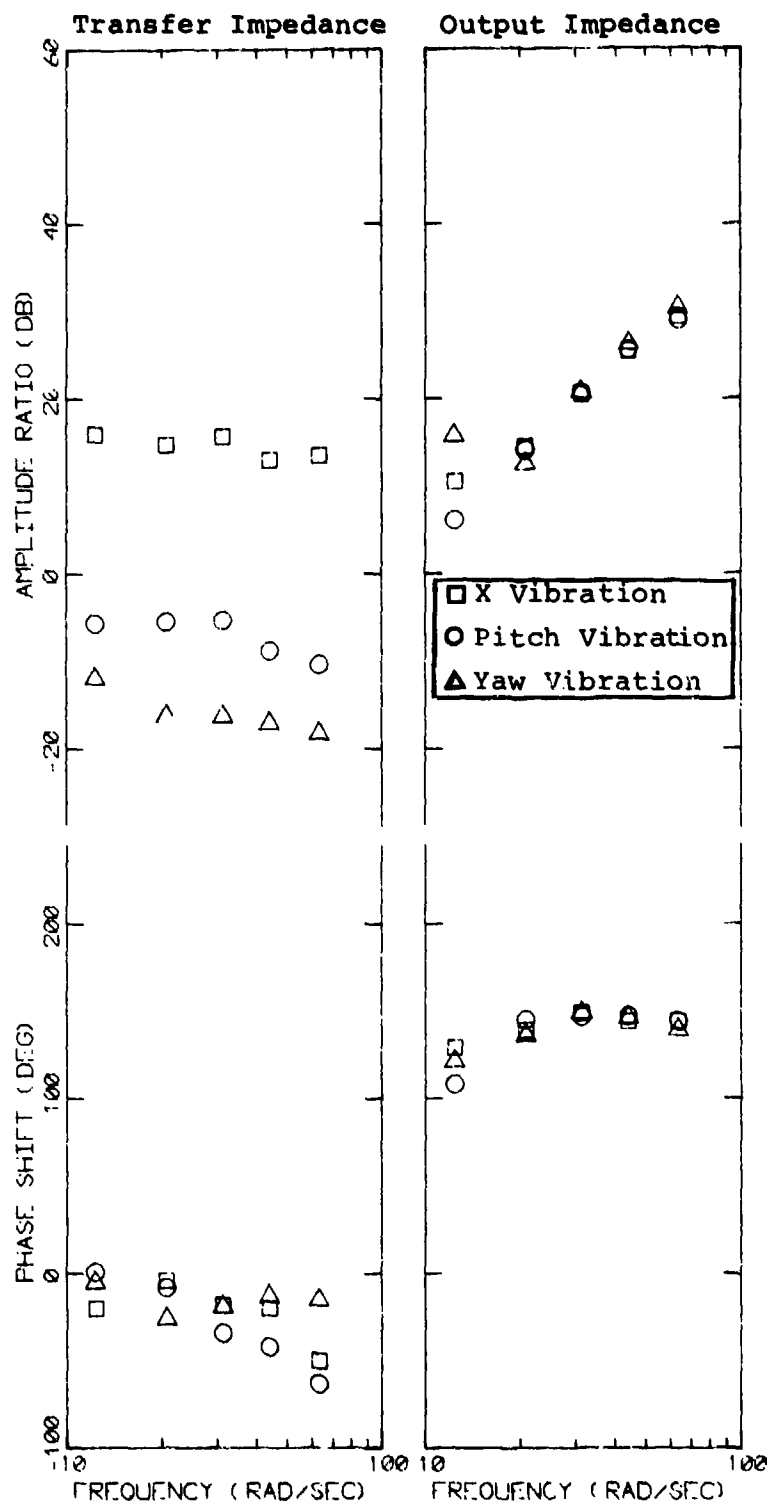


Figure 6. Feedthrough Impedances for Y-Axis Platform Vibration

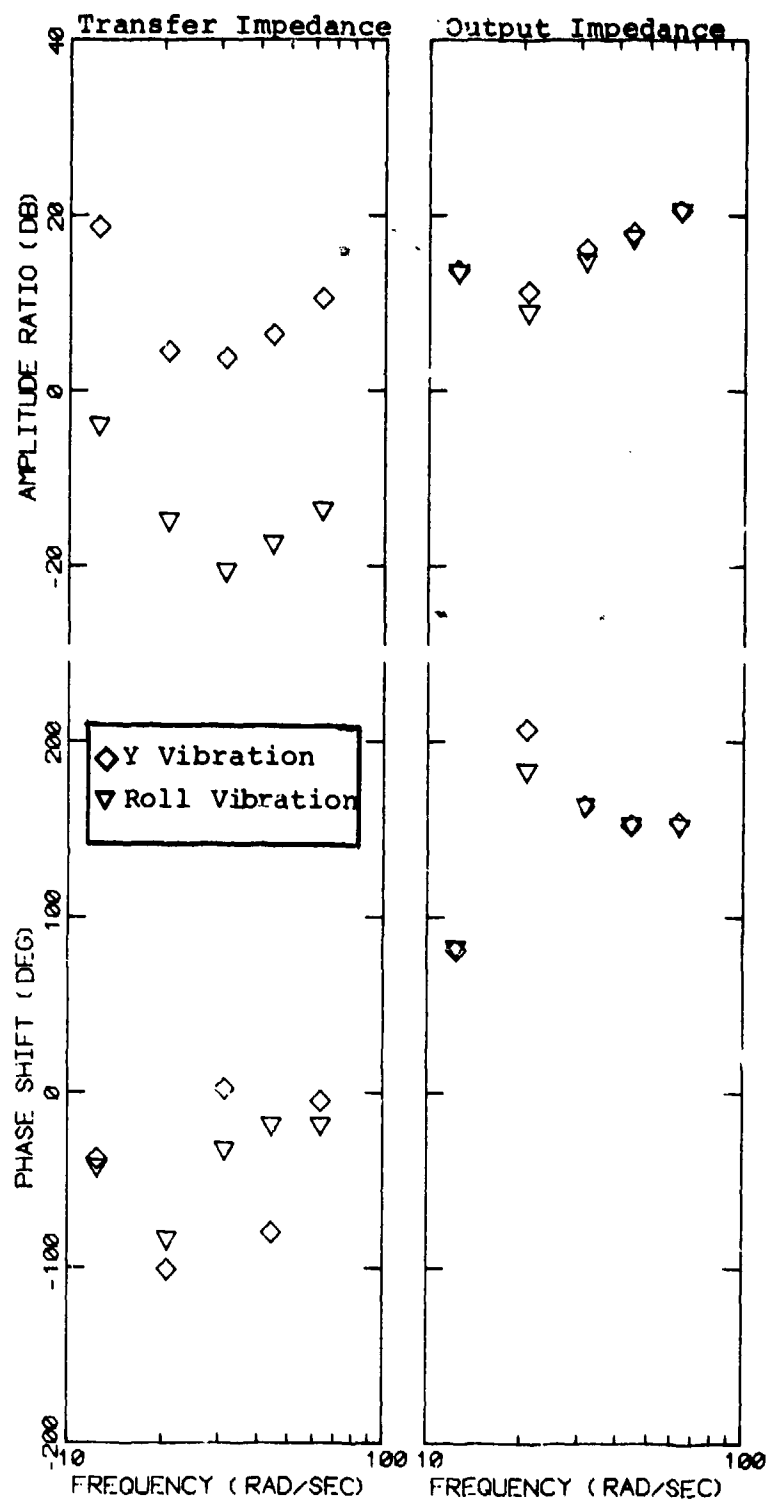
0 dB = 1 pound/g for transfer impedance

0 dB = 1 pound/inch for output impedance



WHL-362

Figure 7. Feedthrough Impedances for X, Pitch, and Yaw Platform Vibrations, Pitch Tracking Task
 0 dB = 1 pound/g for transfer impedance for translational platform vibration
 0 dB = 1 pound/(rad/sec)² for transfer impedance for rotational platform vibration
 0 dB = 1 pound/inch for output impedance



WHL-363

Figure 8. Feedthrough Impedances for Y and Roll Platform Vibrations, Roll Tracking Task

0 dB = 1 pound/g for transfer impedance for translational platform vibration

0 dB = 1 pound/(rad/sec²) for transfer impedance for rotational platform vibration

0 dB = 1 pound/inch for output impedance

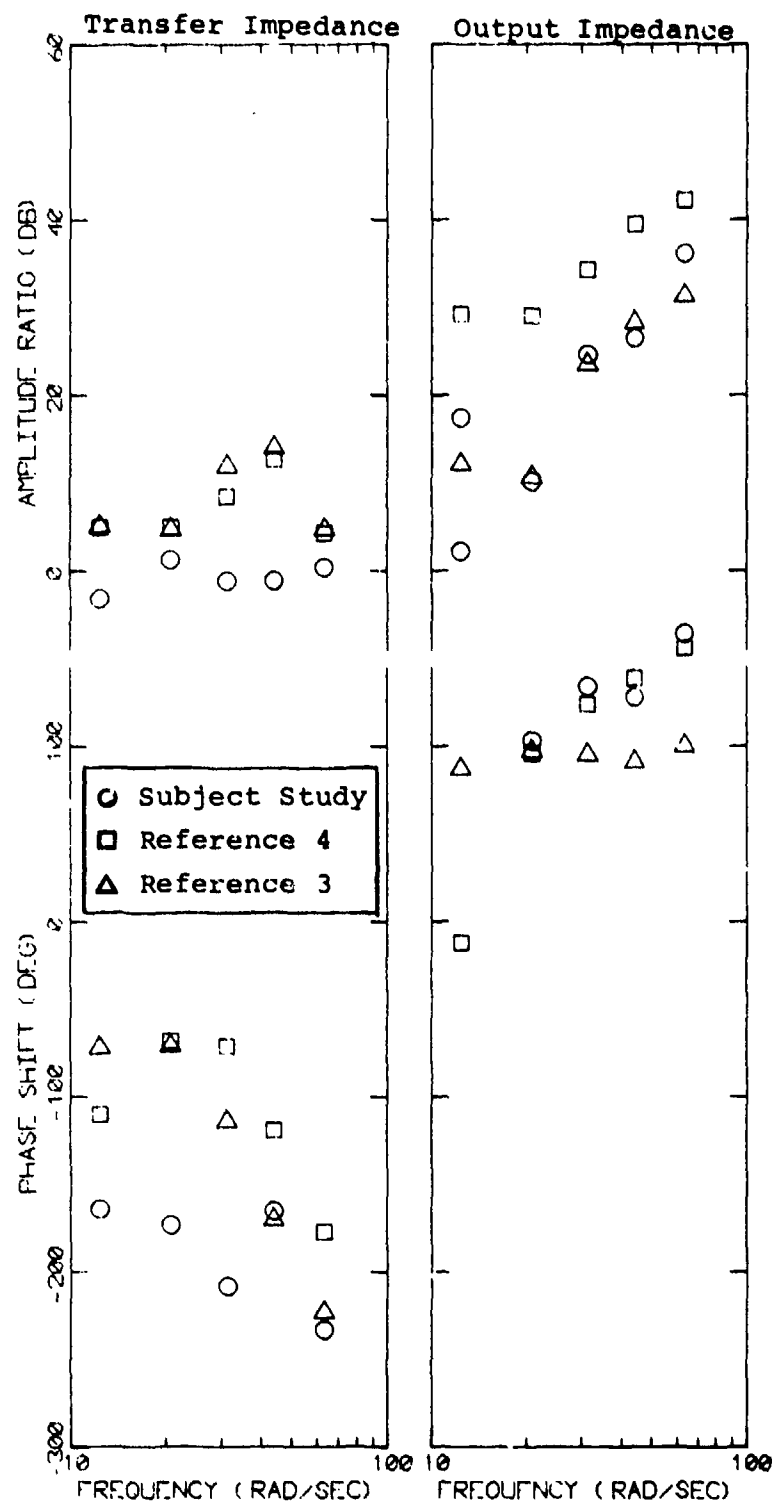
These results imply that the mechanical impedance of the biomechanical linkage as seen from the location of the stick is approximately an inertia for fore-aft motions and viscous damping for left-right motions. Differences in these impedances are not unexpected, as different masses, inertias, pivot points, and neuromuscular systems are involved for different motions. Operationally, the lower output impedance found for the roll axis implies that vibration feedthrough will be greater in this axis for relatively free-moving control sticks, especially at the higher vibration frequencies.

These results are generally consistent with the results of Allen, Jex, and Magdaleno, who found that maximum biomechanical response occurred at lower frequencies for lateral-axis coupling than for couplings along other axes [1]. Nevertheless, the feedthrough response to Z-axis platform vibration differs somewhat from the response behavior observed in earlier studies. Figure 9 compares feedthrough impedances for three successive studies of vibration and tracking, including this study (the "subject study"). The transfer impedances observed in the two earlier studies showed a distinct resonance in the vicinity of 7 Hz, whereas the transfer impedance measured in the subject study is nearly uniform with frequency. The output impedances all show the same high-frequency changes with frequency, although there appear to be some differences in scale factor.

The reasons for the differences shown in Figure 9 are not clear. The biomechanical configuration was essentially the same for all three studies, and the data shown in this figure correspond to nearly identical vibration conditions. The known differences were (1) stick electrical gain, (2) magnitude of the tracking input, and (3) subject population.* Experimental parameters for the three studies are compared in Table 7.

It is possible that stick gain and tracking input influence the way the subject grips the control stick; otherwise, it is not clear how these variables would affect feedthrough impedances, as they do not relate directly to the mechanical coupling between platform and control input. Because stick feedthrough response is highly variable from subject-to-subject (much more so than tracking response), differences in subject populations may account for some of the differences. Figure 10 shows that the transfer impedances for subjects showing maximal and minimal stick feedthrough in the subject study differed by close to 10 dB at the higher vibration frequencies. Neither subject, however, showed the same resonance phenomena observed in the preceding studies. We cannot, therefore, attribute the observed response differences to a particular set of experimental factors with a high degree of confidence, and we suggest that a controlled experiment be performed to systematically explore the effects of task parameters such as control gain, display gain, and tracking input amplitude on feedthrough impedances.

*Stick location (center or side) also differed across studies. However, the study of Levison and Houck [4] showed that stick location had little effect on stick feedthrough.



WHL-365

Figure 9. Feedthrough Impedances for Z-Axis Vibration from Three Study Programs

0 dB = 1 pound/g for transfer impedance
0 dB = 1 pound/inch for output impedance

Table 7

Comparison of Experimental Parameters for Three Studies

Parameter	Reference 3		Reference 4		Subject Study	
	Stiff Stick	Spring Stick	Stiff Stick	Spring Stick	Stiff Stick	Spring Stick
Stick Gain (volts/pound)	0.9	0.36	0.5	1.0	0.9	0.36
Stick Gain (volts/inch)	117	2.5	65	7.5	117	2.5
Spring Gradient (pounds/inch)	130	7.0	130	7.5	130	7.0
Display Gain (inches/volt)	0.19		0.38		0.38	
Rms Tracking Input (volts)	0.64		0.64		2.0	

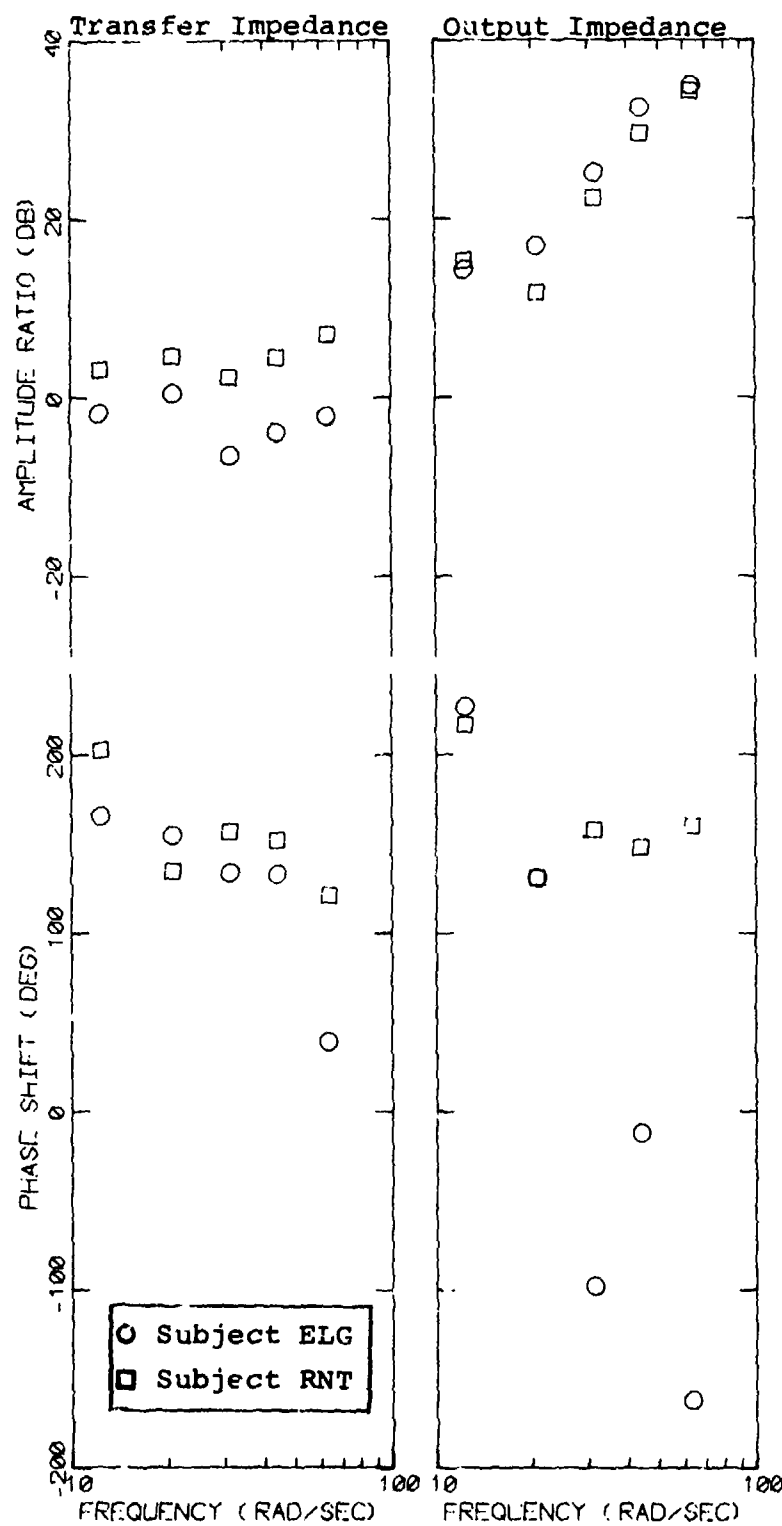
For all studies, system dynamics were

$$E(s) = \frac{4}{s} C(s) + \frac{2}{s} I(s)$$

where $E(s)$ = tracking error, volts

$C(s)$ = control input, volts

$I(s)$ = tracking input, volts



WHL-364

Figure 10. Feedthrough Impedances for Two Subjects, Z-Axis Platform Vibration, Pitch Tracking Task
 0 dB = 1 pound/g for transfer impedance
 0 dB = 1 pound/inch for output impedance

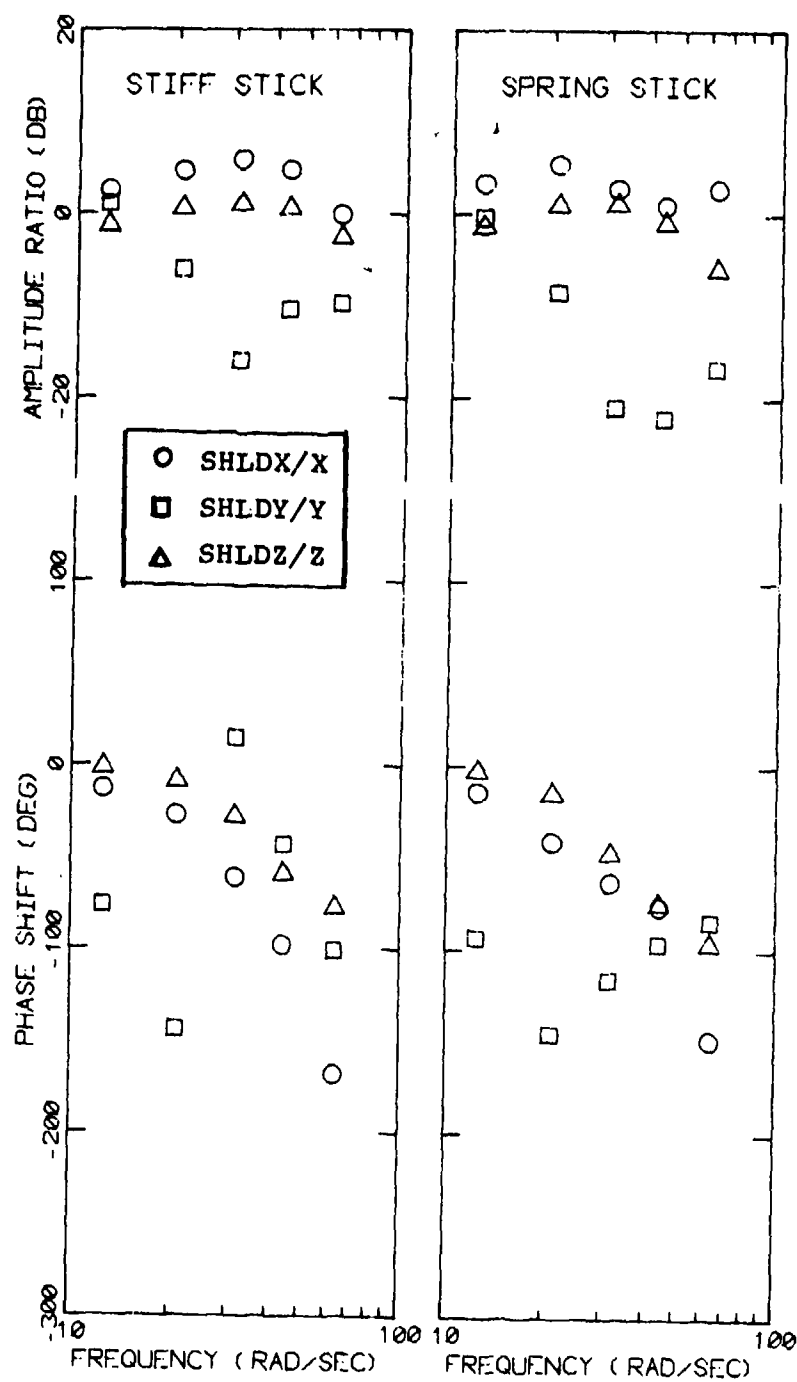
3.1.3 Shoulder Transmissibility

Selected shoulder/platform describing functions are given in Figures 11 through 15. Since the axis of tracking had negligible effect on shoulder/platform transmissibility, all describing functions shown in these figures have been computed from data obtained during pitch-axis tracking. A complete set of describing-function data for shoulder and elbow response are contained in Tables A4-A7 in the Appendix.

Figure 11 shows the direct-coupled transfers for translational platform accelerations. X- and Z-axis transmissibilities are largely similar in form and show a modest resonance effect in the region of 3-5 Hz, with the X-axis transfer showing greater overall magnitude. The Y-axis response, on the other hand, is greatest at the lowest vibration frequency (2 Hz) and decreases with increasing frequency.

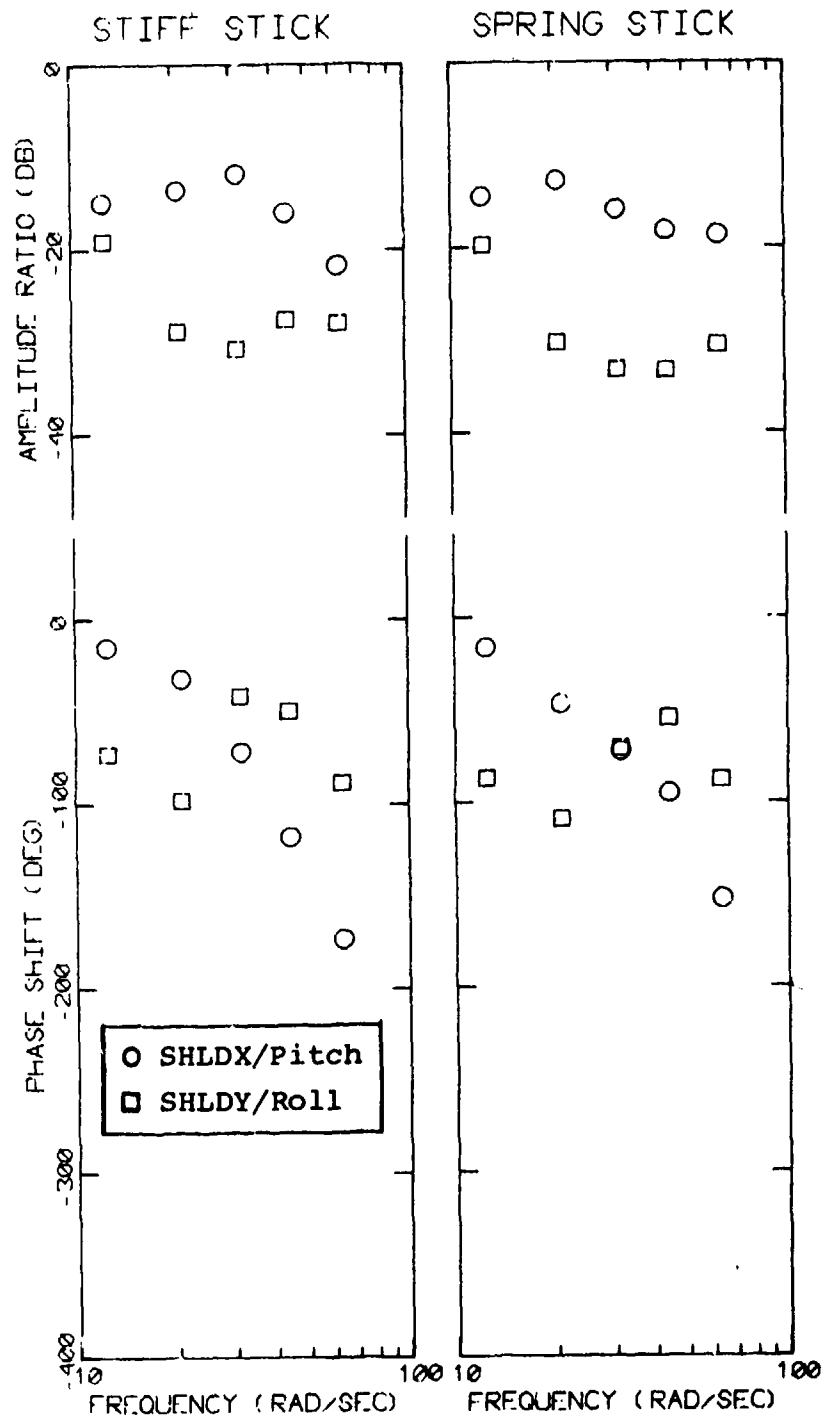
Except for the dip in the Y-axis amplitude ratio, the trends of the Y- and Z-axis results agree with the results obtained in an earlier study of lateral and vertical vibration [1]. Because the Y-axis response was obtained by subtracting two describing functions from a third (see Section 2.4.2), the dips in Figure 11 are suspect and may reflect errors incurred in subtracting quantities that are very close in magnitude.

Shoulder-X/Pitch and shoulder-Y/Roll describing functions are given in Figure 12. Except for a sizeable difference in scale factor, these transfers are similar in form to the Shoulder-X/X and Shoulder-Y/Y describing functions shown in the preceding figure.



WHL-367

Figure 11. Shoulder/Platform Describing Functions for translational Platform Vibration
0 dB = 1 g/g



WHL-374

Figure 12. Shoulder/Platform Describing Functions for Rotational Platform Vibration
 0 dB = 1 g/(rad/sec²)

Direct- and cross-coupled describing functions relating each axis of shoulder response to each translational axis of platform vibration are shown in Figure 13 through 15. The magnitudes of the transfers are greatest for the direct-coupled transfers for X- and Z-axis vibration inputs, which findings support the conclusion that direct-coupled response paths have a higher degree of linear correlation than cross-coupled paths.

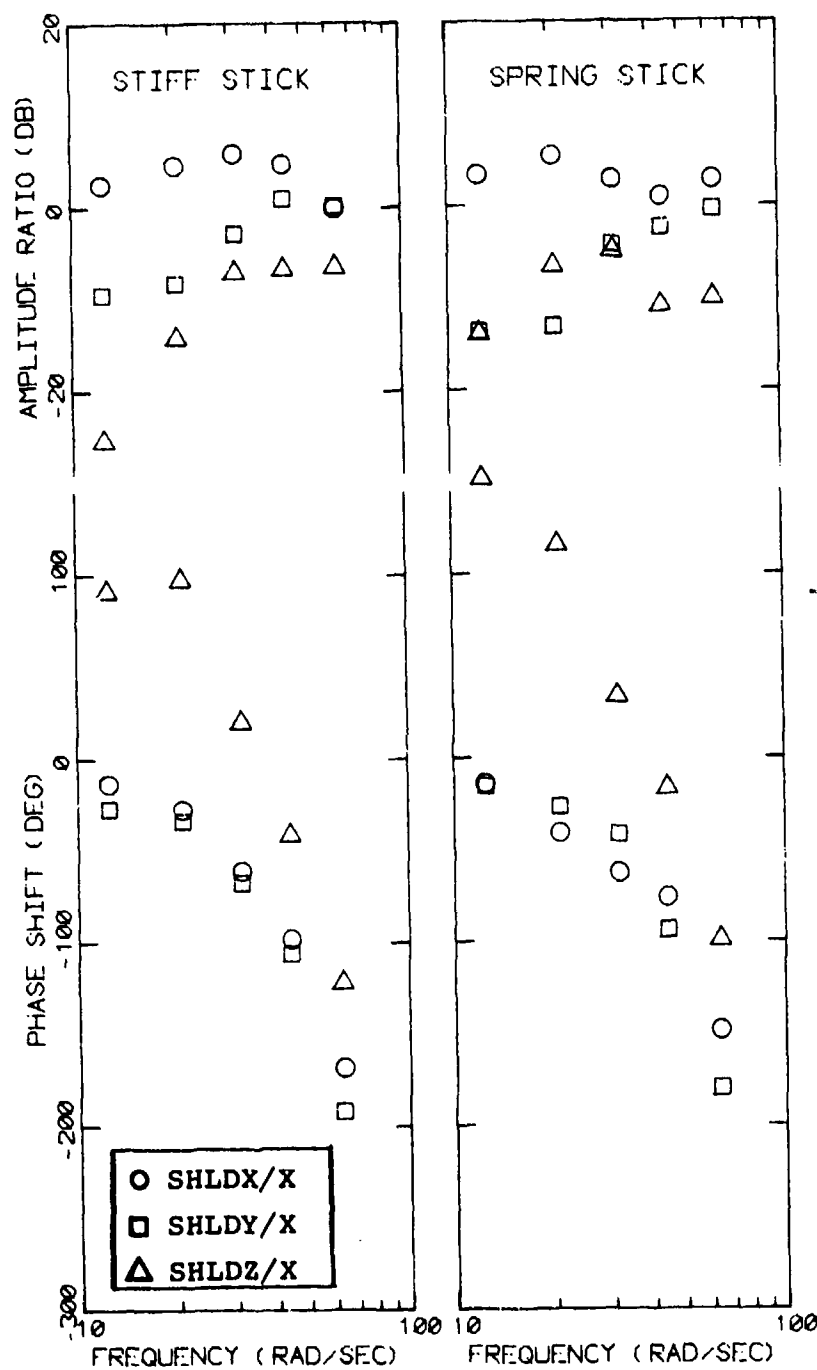
Y-axis platform vibration, on the other hand, appears to introduce about as much platform-correlated response in the X-axis as in the Y-axis. Apparently, Y-axis vibration causes a twisting motion of the torso, which results in both X- and Y-axis shoulder acceleration. (The twisting motion was most likely caused by the fact that one of the subject's hands was anchored to the side-mounted control stick, whereas the other was free to move about.)

3.2 Tracking Behavior

3.2.1 Rms Performance Scores

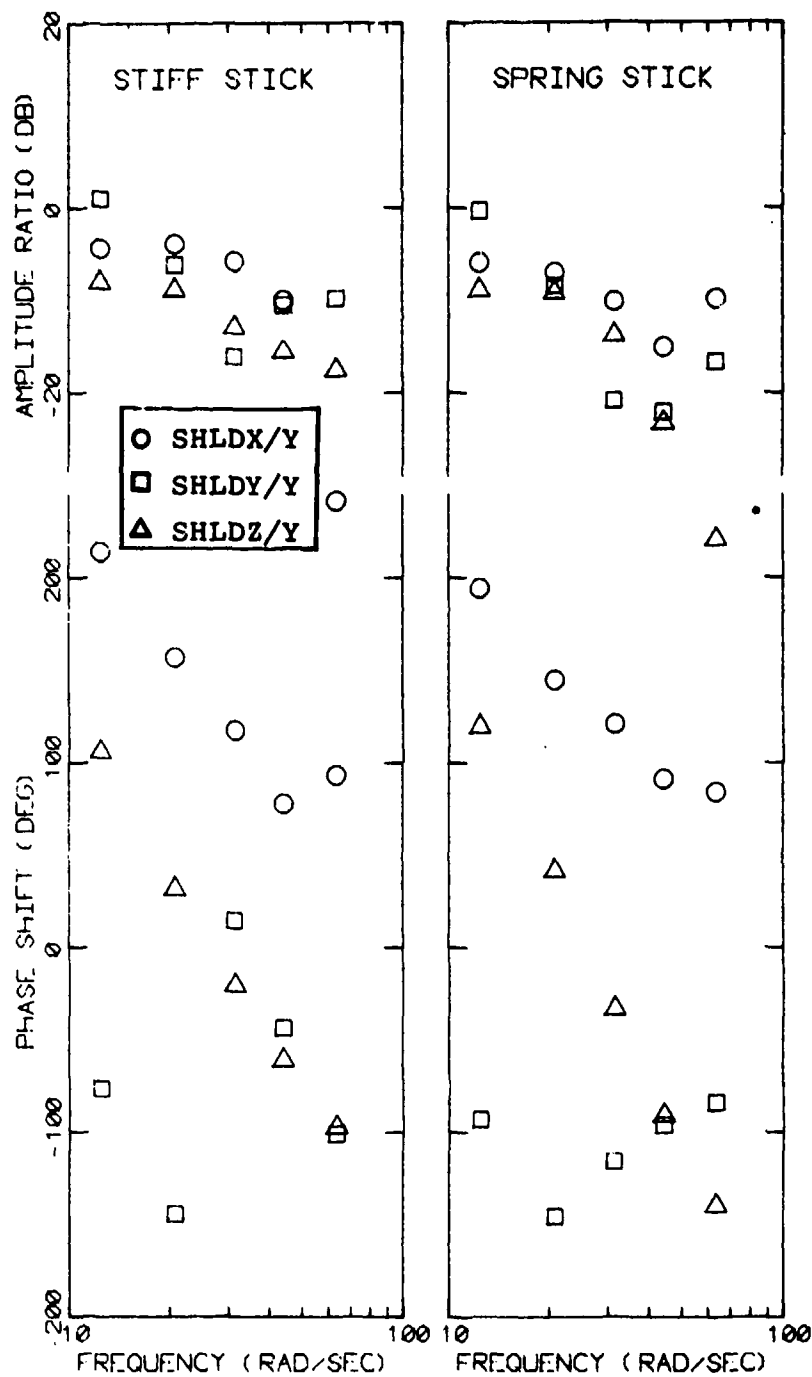
The effect of vibration on rms error and control scores are shown in Figures 16 and 17 for the pitch-axis and roll-axis tracking tasks, respectively. Tabulated scores are given in Table A8 of the Appendix.

The effects of vibration on error scores were relatively small, (maximum increase of about 20%). As found in previous studies [1-4], vibration-static differences were greater for the stiff-stick configuration. X+pitch and pitch platform vibration induced the greatest increase in rms error for the pitch-axis tracking task, whereas all three vibration conditions



WHL-368

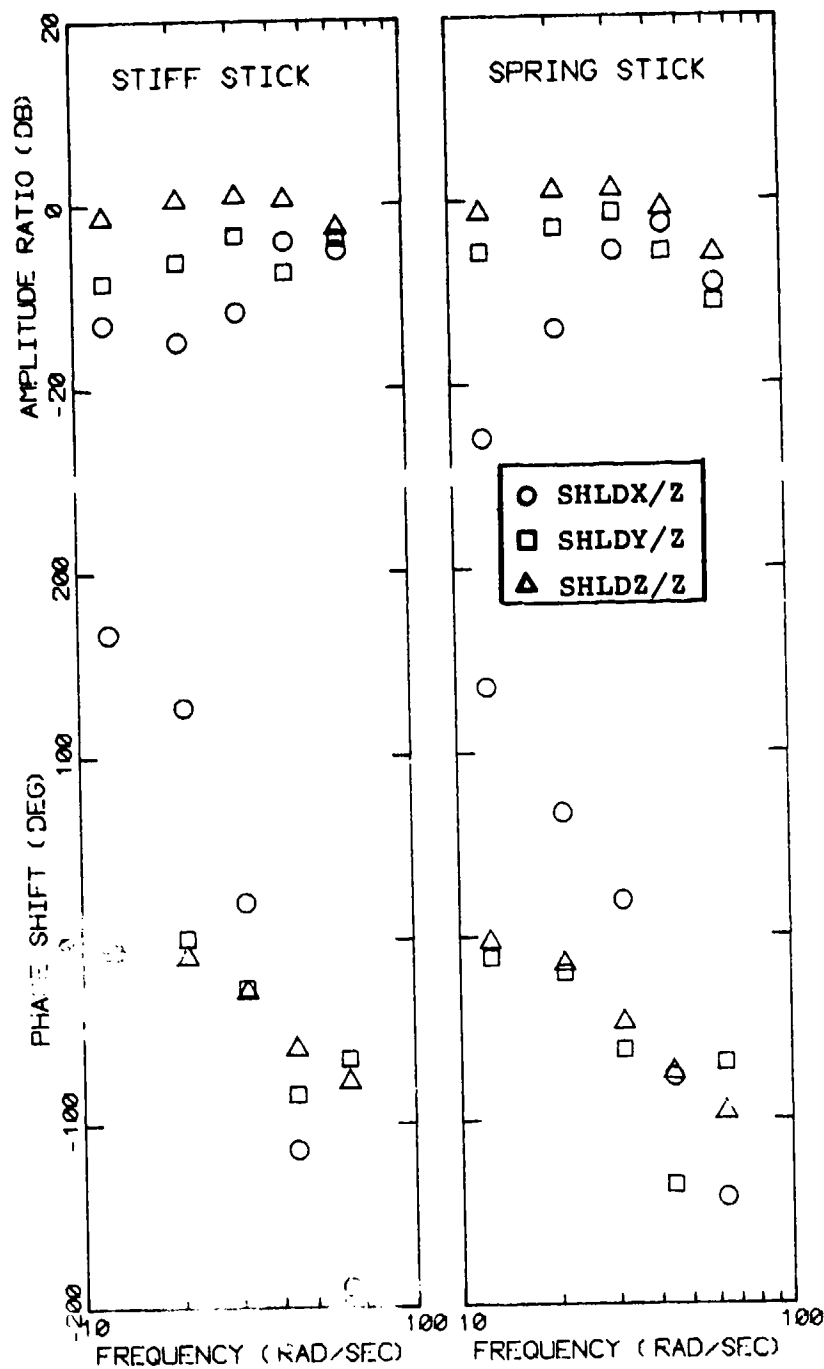
Figure 13. Shoulder/Platform Describing Functions for X-Axis Platform Vibration
0 dB = 1 g/g



WHL-369

Figure 14. Shoulder/Platform Describing Functions for Y-Axis Platform Vibration

0 dB = 1 g/g



WHL-370

Figure 15. Shoulder/Platform Describing Functions for Z-Axis
Platform Vibration
0 dB = 1 g/g

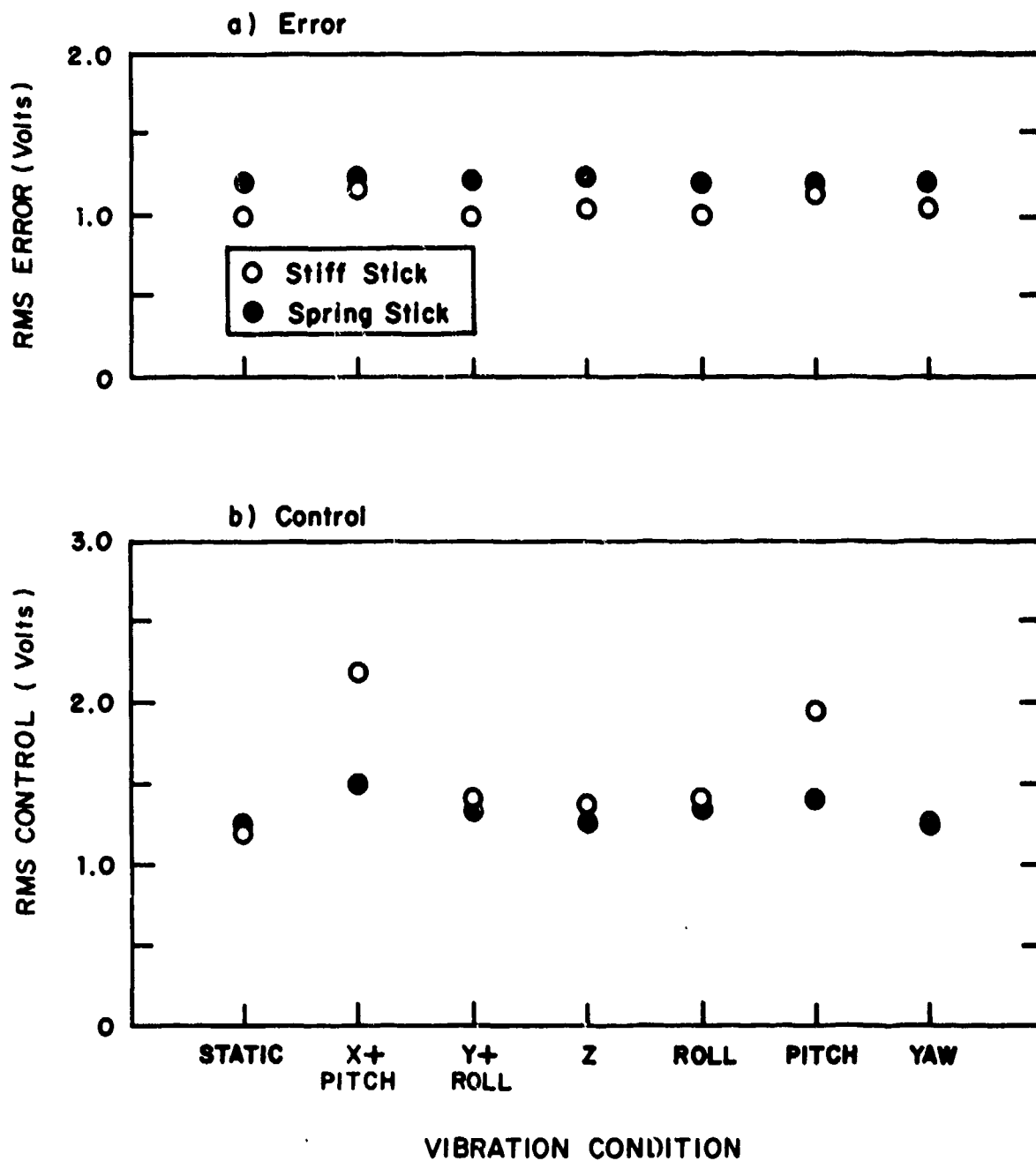


Figure 16. Effect of Vibration on Rms Tracking Performance Scores, Pitch Task

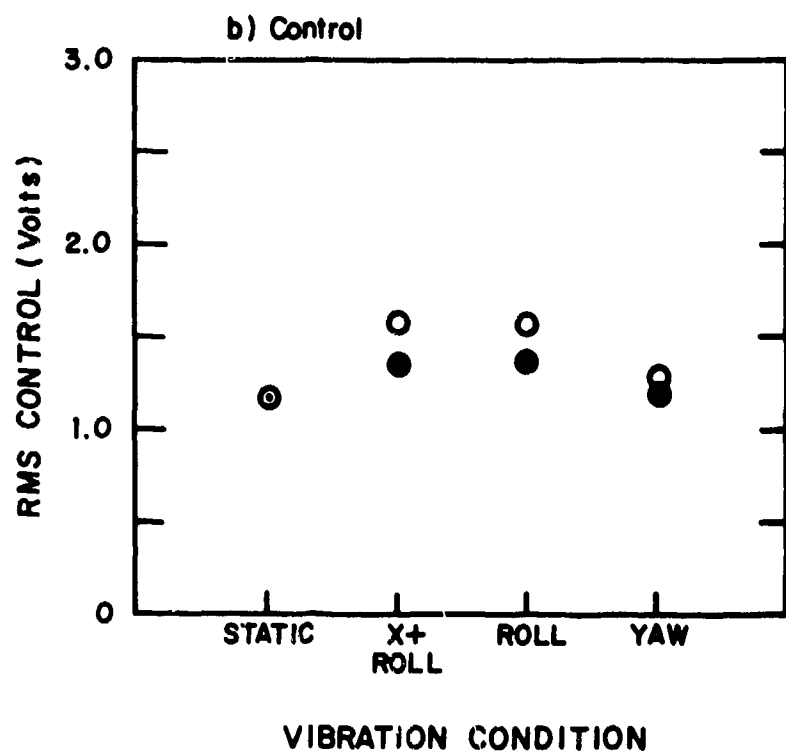
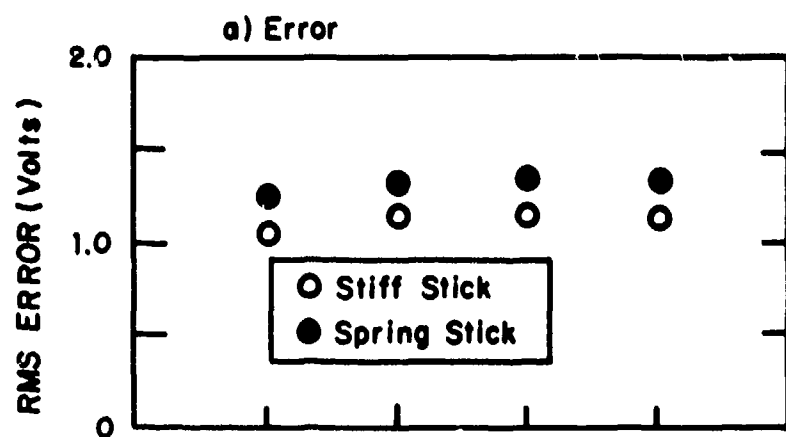


Figure 17. Effect of Vibration on Rms Tracking Performance Scores, Roll-Task

explored for the roll-axis task (Y+roll, roll, and yaw) had roughly the same effect.

Because of the greater degree of stick feedthrough associated with the stiff-stick configuration, the influence of vibration on rms control score was greater for this control configuration. Greatest effects were found for the X+pitch and pitch vibration conditions (pitch tracking task) and for the Y+roll and roll vibration conditions (roll tracking task). These results are consistent with the trends observed for stick feedthrough and shoulder transmissibility.

Table 8 summarizes the results of t-tests on vibration/static differences for each tracking task (Tables 8a and 8b), as well as tests conducted on differences between pitch tracking and roll tracking for a given vibration condition (Table 8c). For the stiff-stick configuration, all of the vibration/static differences in rms control were significant, as were most of the differences in rms error. The effects of vibration on control score were also generally significant for the spring-stick configuration, although changes in rms error were largely not significant for this configuration.

In the static condition, performance on the roll-axis tracking task was not significantly different from performance on the pitch-axis task. Differences across task were generally significant in vibration environments, however. Inspection of Figures 16 and 17 show that roll-axis scores were generally greater than corresponding pitch-axis scores for the vibration conditions common to both tracking tasks (Y+roll, roll, and yaw). This trend was expected, since the side-to-side control motions required for roll-axis tracking were more highly coupled to the

Table 8
Results of T-Tests of Tracking Scores

Vibration Condition	Stiff Stick		Spring Stick	
	Error	Control	Error	Control

a) Effect of Vibration, Pitch Task

X	.001	.001	-	.001
Y	-	.001	-	.05
Z	.001	.01	-	-
Roll	-	.001	-	.05
Pitch	.001	.001	-	.001
Yaw	.05	.001	-	-

b) Effect of Vibration, Roll Task

Y	.05	.001	-	.001
Roll	.05	.001	.05	.001
Yaw	-	.01	.05	-

c) Effect of Tracking Task (Pitch vs Roll)

Static	-	-	-	-
Y	.001	.01	.01	-
Roll	.001	.01	.001	-
Yaw	.05	-	.001	-

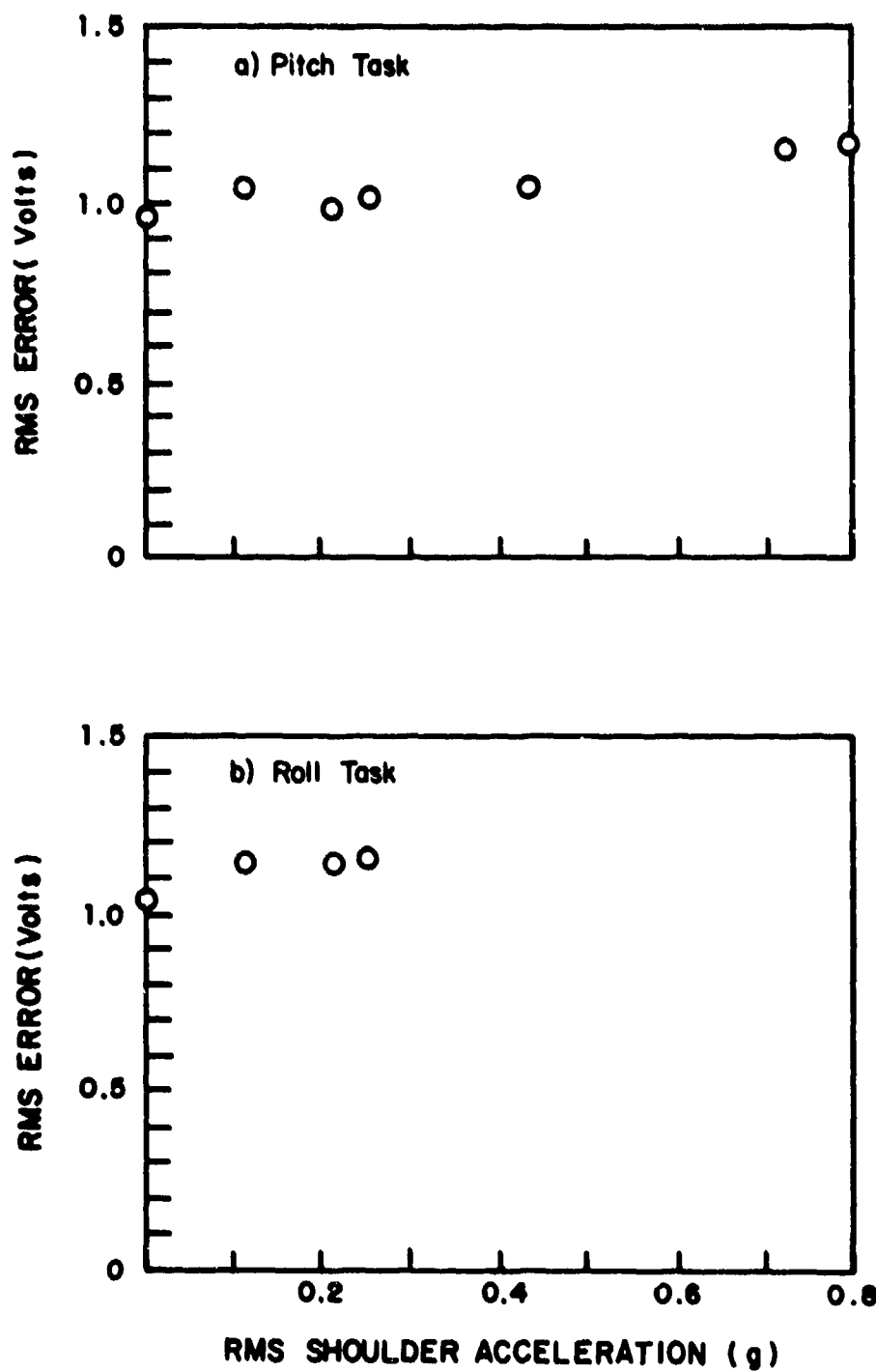
platform motions than the fore-aft motions required for pitch-axis tracking.

Figure 18 shows that rms tracking error tended to increase with rms shoulder acceleration. (These results are for the stiff-stick configuration.) This trend supports the hypothesis, proposed in an earlier study [4], that shoulder acceleration is an important factor in performance degradation caused by whole-body vibration. This relationship is discussed further in Section 3.3.

3.2.2 Frequency Response

Average frequency-response measures for selected conditions are given in Figures 19 through 21. These measures include the pilot describing function (amplitude ratio and phase shift) as well as the ratio of remnant-related control power to input-correlated control power ("rem/cor"). Frequency-response data for all experimental conditions are contained in Tables A9 and A10 of the Appendix.

The effects of vibration on frequency-response measures were similar to those observed previously: (1) amplitude ratio was reduced slightly at low frequencies and increased at the highest measurement frequency of 10.5 rad/sec; (2) phase lag increased at the highest measurement frequencies, and (3) the ratio of remnant to correlated control power increased. T-tests of paired differences (summarized in Tables A11 and A12 of the Appendix) revealed that vibration/static differences were generally significant at the highest two measurement frequencies.



WHL-357

Figure 18. Relation Between Rms Tracking Error and Rms Shoulder Acceleration

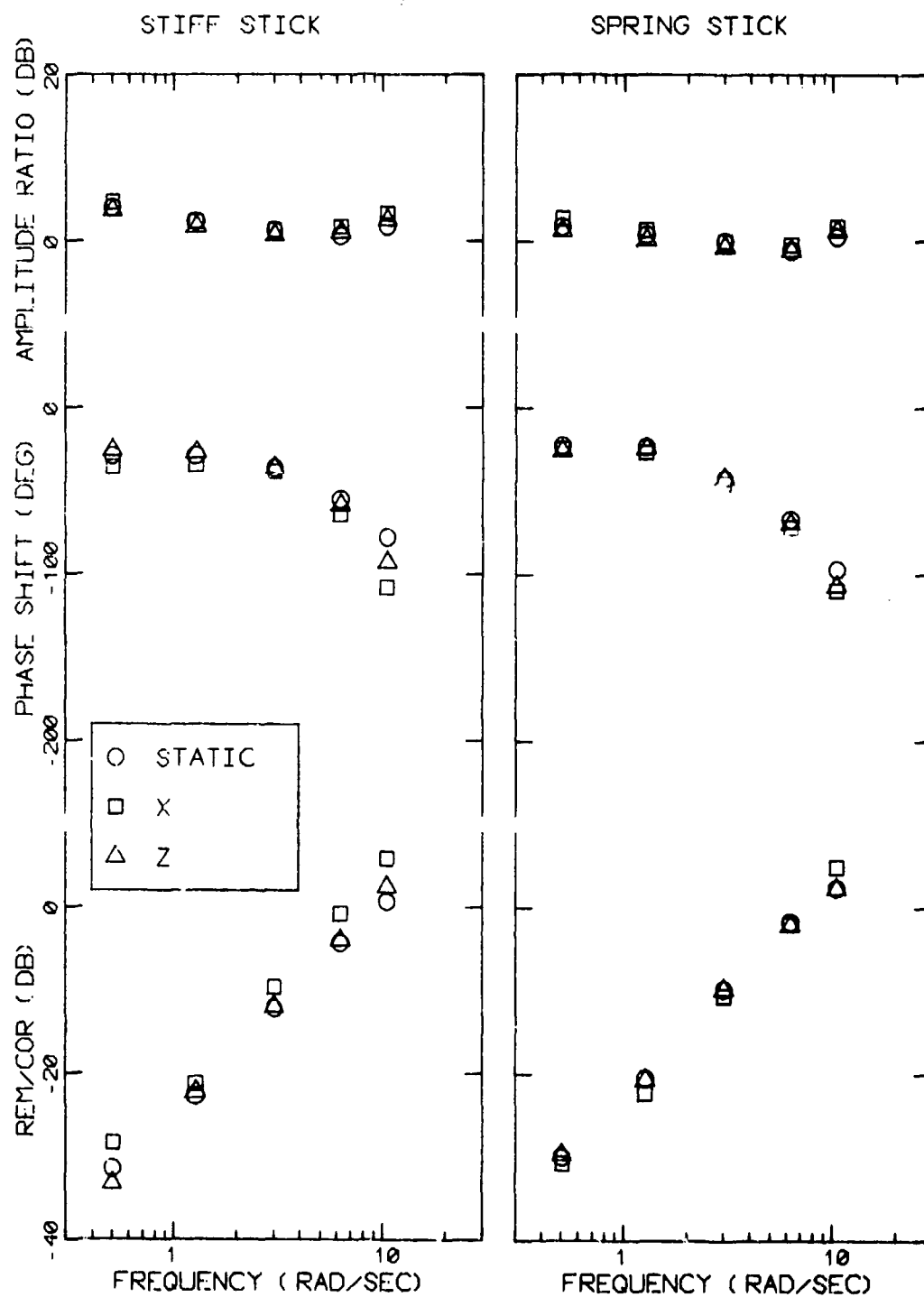
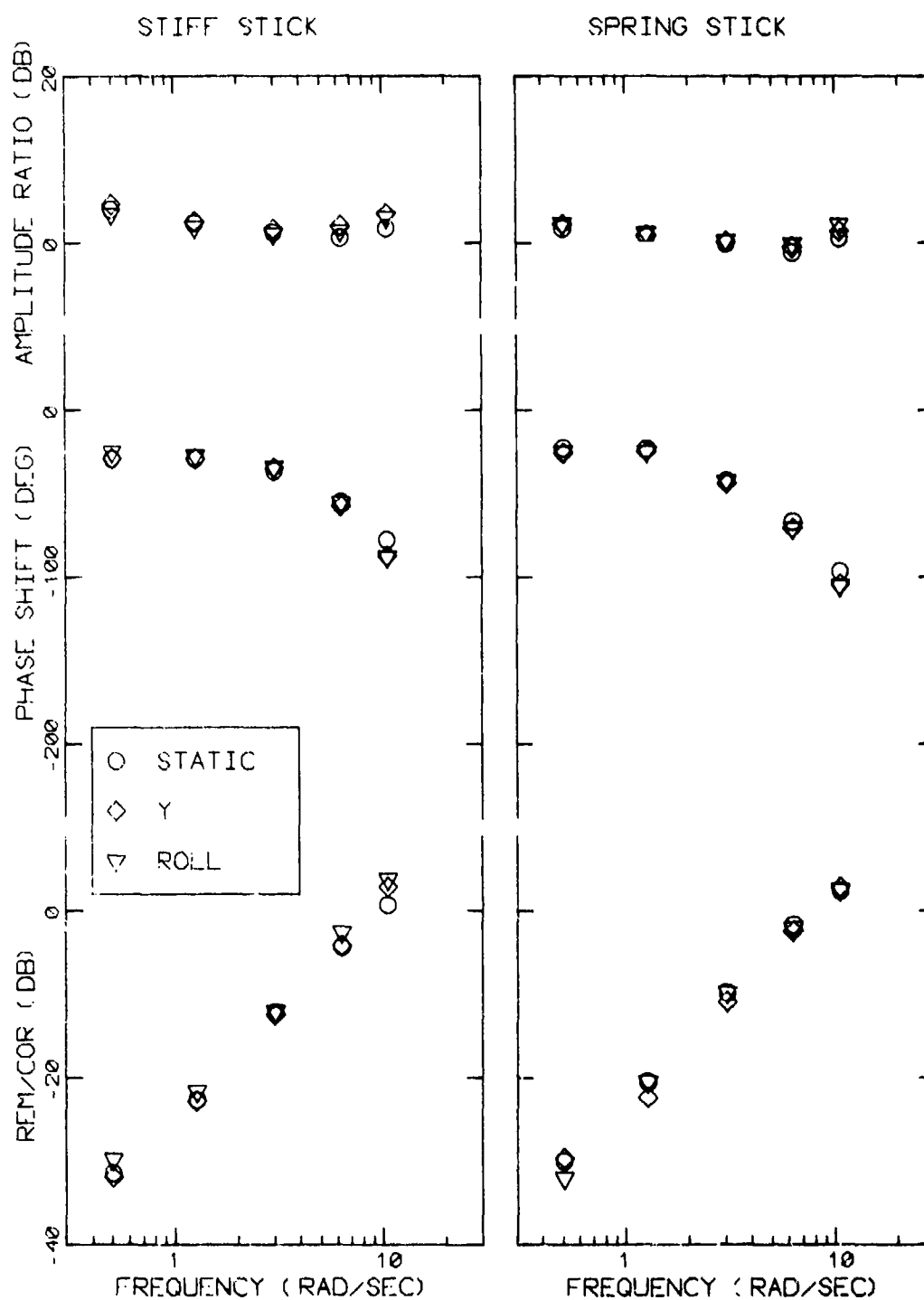


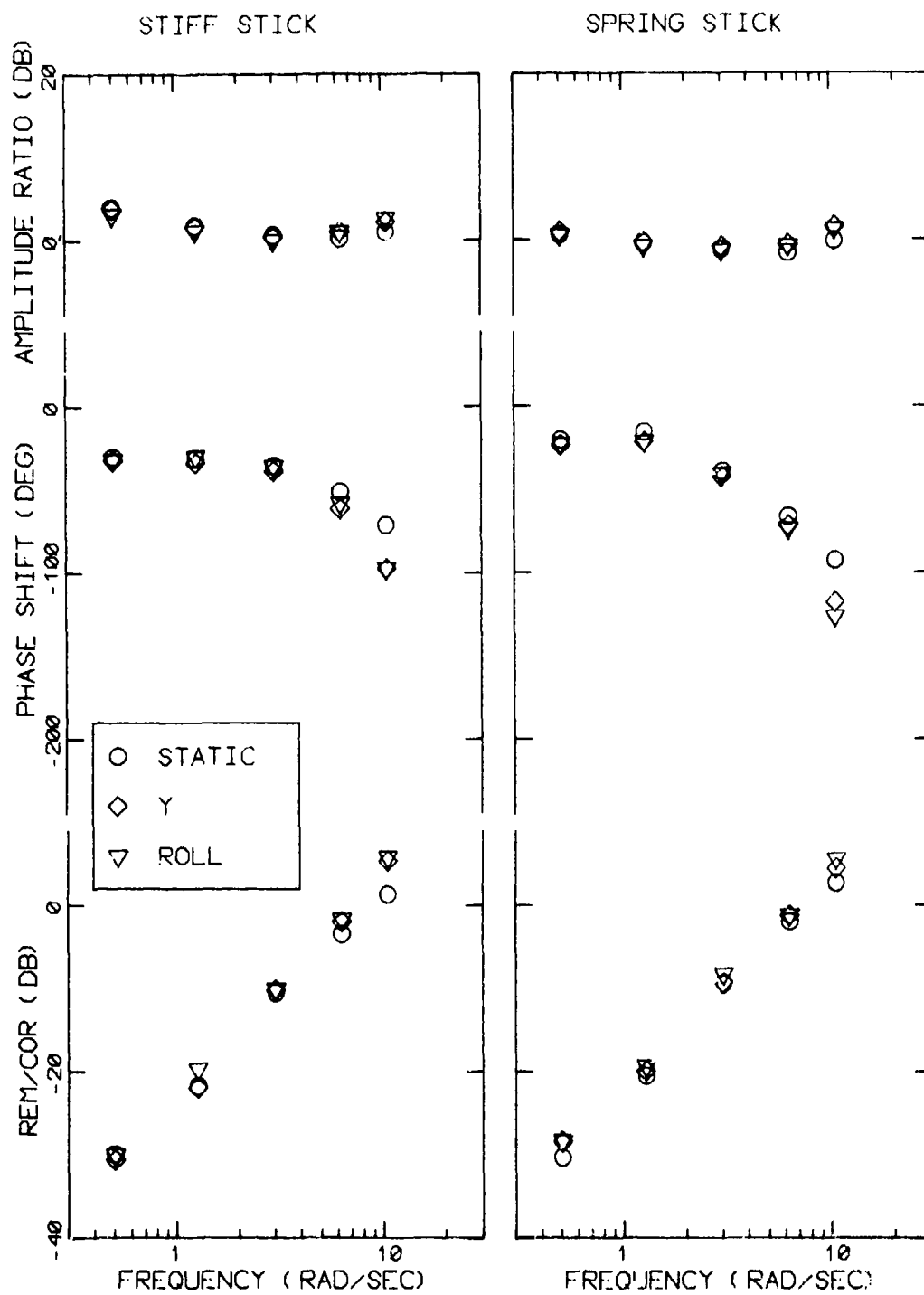
Figure 19. Effect of Longitudinal-Axis Platform Vibration on Pilot Frequency Response, Pitch Task

WHL-375



WHL-376

Figure 20. Effect of Lateral-Axis Platform Vibration on Pilot Frequency Response, Pitch Tracking Task



WHL-377

Figure 21. Effect of Lateral-Axis Platform Vibration on Pilot Frequency Response, Roll Tracking Task

A comparison of Figure 20 with Figure 21 shows that lateral-axis vibration inputs had a greater effect on pilot frequency response for the roll-axis tracking task than for the pitch task, especially at the higher measurement frequencies. T-tests showed that many of these differences were statistically significant (Table A13). Thus, vibration inputs in the axis of control response appear to have a greater influence on pilot response behavior than do vibration inputs acting orthogonally to the axis of control response. This effect is in addition to the greater feedthrough associated with colinear vibration inputs and has implications concerning the relationship between pilot-related model parameters and biodynamic response, as discussed in Section 3.3.

3.2.3 Comparison with Previous Studies

Z-axis vibration had less of an influence on tracking performance than did similar vibration environments in previous studies. The influence of feedthrough was expected to be less because of the larger rms tracking input used in the subject study. With the effects of feedthrough discounted, however, performance decrements were still less for this study.

Figure 22 compares the ratio of rms performance in a vibration setting to performance in the static case for three study programs. In order to allow a comparison of tracking capabilities that is not confounded by the direct effects of biomechanical feedthrough, ratios are based on performance scores that have been adjusted to remove the influence of stick feedthrough. All data pertain to similar Z-axis vibration environments and similar stick configurations.*

*Electrical stick gain was varied from study-to-study, but spring constants, damping ratios, and stick masses were roughly the same.

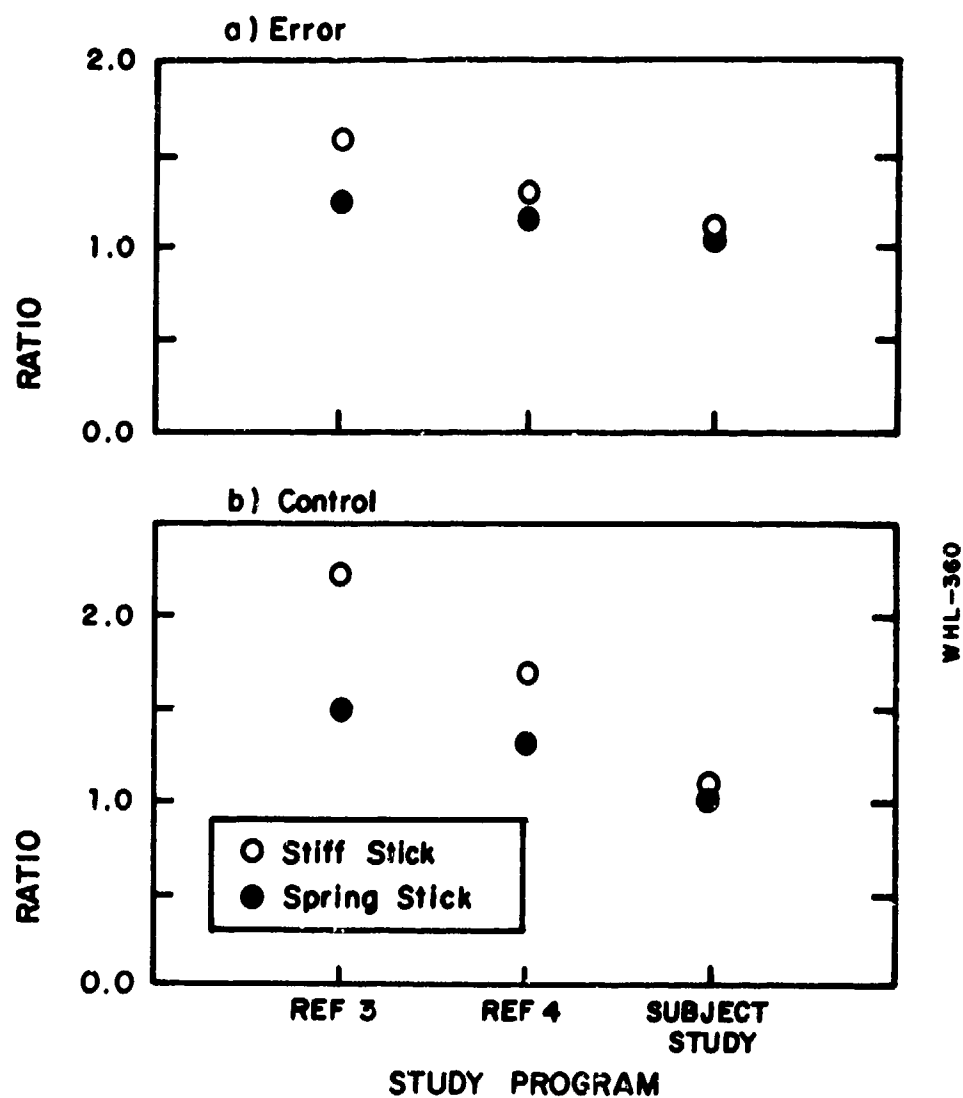


Figure 22. Ratios of Rms Performance in a Z-Axis Vibration Environment to Rms Performance in a Static Environment

These results do not support the model that has recently been proposed for describing the effect of vibration on pilot-related model parameters [4]. In this model, both time delay and motor noise/signal ratio are assumed to vary linearly with rms shaker acceleration. Since the biodynamic environment was the same in the three studies compared in Figure 22, time delay and motor noise should be invariant, and tracking performance (discounting the effects of stick feedthrough) should be nearly identical. In order to account for the results shown in Figure 22, a revised model for relating vibration parameters to tracking model parameters has been proposed and tested, as described below.

3.3 Model Analysis

3.3.1 Model Structure

Model analysis was applied to experimental results obtained in the subject study as well as in earlier studies to determine a consistent way of relating tracking performance to vibration parameters. The model used in this effort consists of two major submodels: a biodynamic model to predict limb and body motion resulting from vibration, and a pilot/vehicle model to predict tracking performance. A third submodule -- the "interface" module -- relates changes in pilot-related tracking parameters to biodynamic response. This model is similar to the models used in recent studies, the only difference being in the interface module.

The key element of the model is the "optimal-control" model for pilot/vehicle systems developed by BBN [6,7]. This model relates system performance and pilot response to elements of the control system such as plant dynamics, control-stick properties, and

external tracking disturbances. The effects of vibration are represented partly as a direct control input resulting from direct biomechanical coupling to the platform and as changes in values assigned to pilot-related parameters of the basic pilot/vehicle model.

A diagram of the model structure is shown in Figure 23. For simplicity of exposition, we consider a single-input, single-output control system subject to vibration disturbances in a single axis. This model can be readily extended to include multi-input, multi-output systems. The reader is referred to the literature for examples of application of the optimal-control pilot/vehicle model to complex control situations [8-11].

The pilot is assumed to observe a compensatory display of tracking error and to manipulate a single control stick. Because the pilot will generally extract velocity as well as displacement information from the error indicator, tracking error is shown in Figure 23 as a vector quantity. The system is assumed to be disturbed by one or more zero-mean Gaussian random processes "i" which we designate as "tracking inputs" to differentiate from vibration inputs. In laboratory situations, tracking inputs are usually added in parallel with the pilot's control (to simulate wind gusts acting on the vehicle, for example) or in parallel with the vehicle output (i.e., as a command input).

We consider the control input " δ " to be the sum of two components: δ_t , the control input that is intended to minimize tracking error, and δ_v , an input correlated with the platform vibration input α_p that results from biomechanical vibration feedthrough. The signal δ_t includes both the response to the

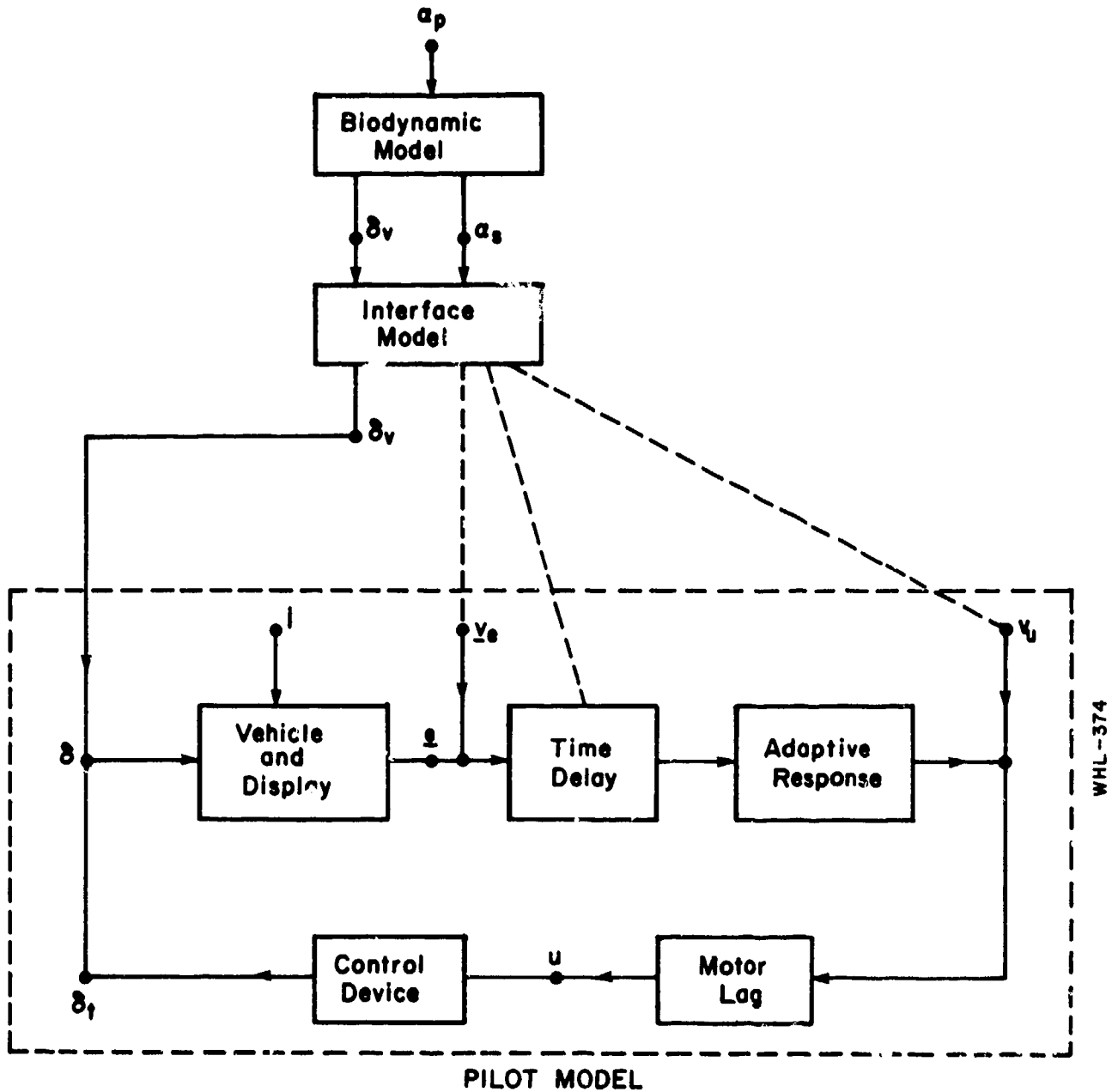


Figure 23. Diagram of the Model Structure

tracking error as well as wide-band stochastic behavior (i.e., "pilot remnant"). The control signal "u" that is actually generated by the pilot is converted to the electrical input " δ_t " in a manner determined by the mechanical and electrical properties of the control device.

Pilot randomness is represented by a set of observation and motor noise processes. The pilot's perceptions of error displacement and error rate are assumed to be perturbed by white noise processes v_e , and an additional motor noise process v_u is assumed to perturb control activity. Other pilot-related limitations include an effective processing delay ("time delay" in Figure 23) associated for convenience with sensory inputs and a first-order low-pass filter ("motor lag") applied to the pilot's control response. Within the constraints imposed by the pilot's perception of the task and by the limitations mentioned above, the pilot will adapt his control strategy to achieve best performance.

Unlike the pilot/vehicle model, which utilized state-variable (i.e., time-domain) descriptions of system behavior, the necessity to rely on empirical frequency-response data dictate that the biodynamic submodule be formulated in the frequency domain. Predictions of rms biodynamic response power (e.g., vibration-correlated control input, shoulder acceleration, etc.) were performed by integrating the following type of expression in the frequency domain:

$$\sigma_x^2 = \int \left| \frac{x}{\alpha_p} \right|^2 \phi_{\alpha_f \alpha_p} d\omega \quad (2)$$

where σ_x^2 is the mean-squared response of the biodynamic variable "x", X/α_p is the empirically-determined describing function relating "x" to platform vibration, and $\phi_{\alpha_p \alpha_p}$ is the spectral density of the platform vibration. (For sum-of-sines vibration inputs, integration was replaced by summation.)

In the case of stick feedthrough, the control/platform transfer function was replaced by the impedance model of equation (1), and control and error variances arising from vibration feedthrough were predicted as follows:

$$\sigma_{c_v}^2 = \int \left| \frac{zT}{zO+zS} \right|^2 K_e^2 \phi_{\alpha_p \alpha_p} d\omega \quad (3)$$

$$\sigma_{e_v}^2 = \int \left| \frac{zT}{zO+zS} \right|^2 K_e^2 |Y_c|^2 \phi_{\alpha_p \alpha_p} d\omega \quad (4)$$

where Y_c is the transfer function of the plant dynamics.

Considerable testing of model predictions against experimental results was required to find a consistent relationship between pilot parameters and biodynamic response parameters that would account for the results obtained in three consecutive studies (including the subject study). The model developed in the preceding study [4] - that of linearly relating motor noise/signal ratio and time delay to shoulder acceleration - did not provide a consistent match to the results of that study and of the subject study. Scale factors that matched the earlier results yielded predicted error and control scores for the subject study that were substantially larger than those obtained experimentally.

This interface model was then modified to let motor noise covariance (rather than noise/signal ratio) vary linearly with rms shoulder acceleration. The revised model also failed to provide accurate performance predictions across studies. Finally, the following relationships were found to provide consistently accurate performance predictions for the various stiff-stick experimental conditions explored in these studies:

$$\begin{aligned} T &= 0.15 + 0.1 \cdot (\alpha_s / \sigma_u) \\ V_u &= 0.02 \cdot (\alpha_s / \sigma_u) \end{aligned} \tag{5}$$

where T is the effective pilot time delay in seconds, V_u is the autocovariance of the (white) injected motor noise process, α_s is rms shoulder acceleration in g's, and σ_u is the predicted rms control force in pounds. The coefficients of 0.1 and 0.02 shown in the above relationship are empirical findings and have no clear theoretical meaning.

If we assume that neuromotor disturbances (other than stick feedthrough) are related to shoulder (or limb) vibration, then a parallel can be made between the form of the relationships shown above and our model for visual thresholds. The threshold model is such that injected observation noise increases as the rms variation of the corresponding display variable decreases relative to the assumed threshold [8, 11]. Similarly, equation (5) implies that the adverse effects of vibration increase as the neuromotor disturbance (signified by shoulder acceleration) increases relative to the "signal" (signified by the control activity generated in tracking). Conversely, this model implies that the effects of vibration can be reduced by manipulating the control gain and/or the tracking signal so as to increase the control forces required for tracking.

The interface model described by equation (5) has been validated only for control situations using a nearly isometric control stick. As discussed below, modifications will be required to model the effects of vibration when control sticks of relatively low force/displacement ratios are employed.

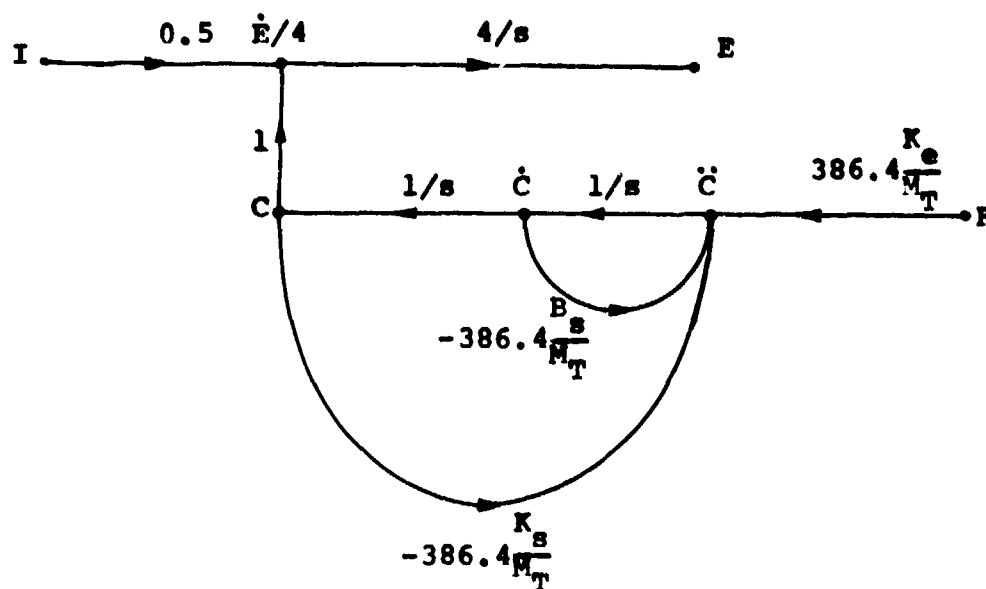
3.3.2 Model Validation

The model described above was used to test the interface submodel described in equation (5) across a variety of experimental conditions. A second-order model of the pilot/stick interface was included in the description of the tracking task, as shown in Figure 24. (The force variable "F" shown in this diagram corresponds to the control variable "u" of the model of Figure 2.)

The following pilot-related model parameters were used for all tests of the model:

- a. Cost functional = $\sigma_e^2 + g \sigma_u^2$, where "g" is selected to yield a "motor time constant" of 0.1 seconds.
- b. Observation noise/signal ratio = -21 dB.
- c. Threshold of error perception = 0.07 volts; threshold on error-rate perception = 0.28 volts.*
- d. Time delay and motor noise determined according to the model of equation (5).

*These thresholds correspond to visual thresholds of 0.05 arc degrees and 0.2 arc degrees/second for displacement and rate perception.



HL-239

- I** = Tracking Disturbance, volts
- E** = Tracking Error, volts
- C** = Control Input, volts
- F** = Applied Force, pounds
- K_e = Electrical Stick Gain, volts/inch
- K_s = Spring Gradient, pounds/inch
- B_s = Stick Damping, pounds/(in/sec)
- M_T = Combined Mass of Stick and Forearm, pounds

Figure 24. Linear Flow Diagram of the Tracking Task

Parameters for the pilot/stick interface (stiff-stick configuration) were:

$$K_e = 117 \text{ volts/inch}$$

$$K_s = 130 \text{ pounds/inch}$$

$$B_s = 0.0103 \text{ pounds/(inch/second)}$$

$$M_T = 15 \text{ pounds}$$

Values for the first three of these parameters were obtained from either adjustment or measurement of the properties of the control stick. The value of 15 pounds associated with the effective mass of the pilot/stick interface was selected on the basis of previous modeling results in which this value was found to provide an acceptable match to both stiff-stick and spring-stick performance measures [4].

Predicted rms shoulder acceleration was computed by performing the frequency-domain integration indicated in equation (2) for each of the three translational axes of shoulder response, then taking a vector combination of these results to yield total rms acceleration. Thus, the predicted rms shoulder accelerations used in the interface model of equation (5) were less than the accelerations determined experimentally, since only vibration-correlated response was considered. Correlations between axes of platform vibration were considered when predicting the effects of simultaneous vibration in two axes, as described in [5].

Figure 25 compares predicted and measured rms error and control score for the static situation (pitch-axis tracking) and for four additional vibration/tracking conditions. These scores represent the combined effects of tracking plus stick feedthrough.

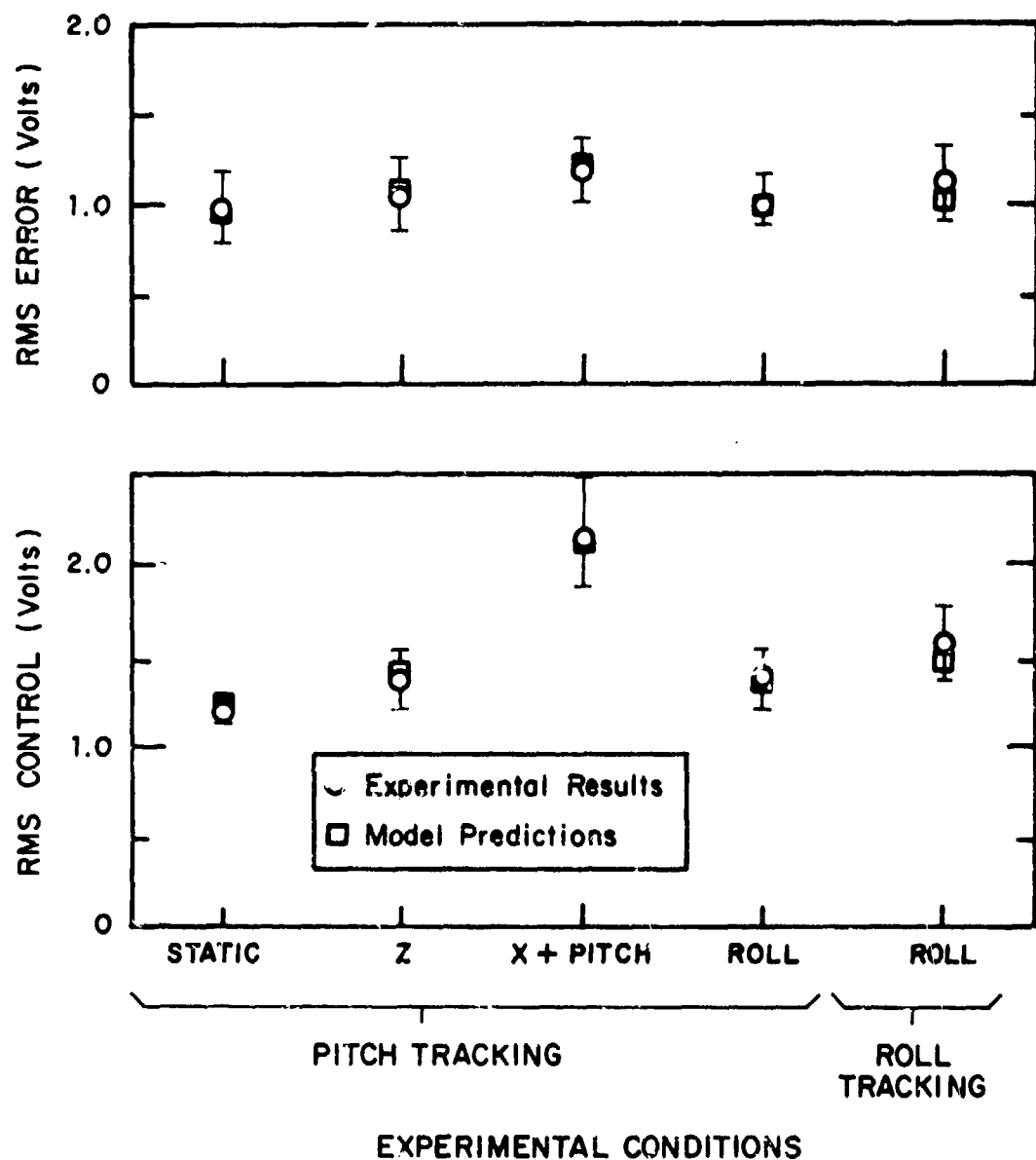


Figure 25. Comparison of Predicted and Measured Rms Performance Scores for Five Experimental Conditions

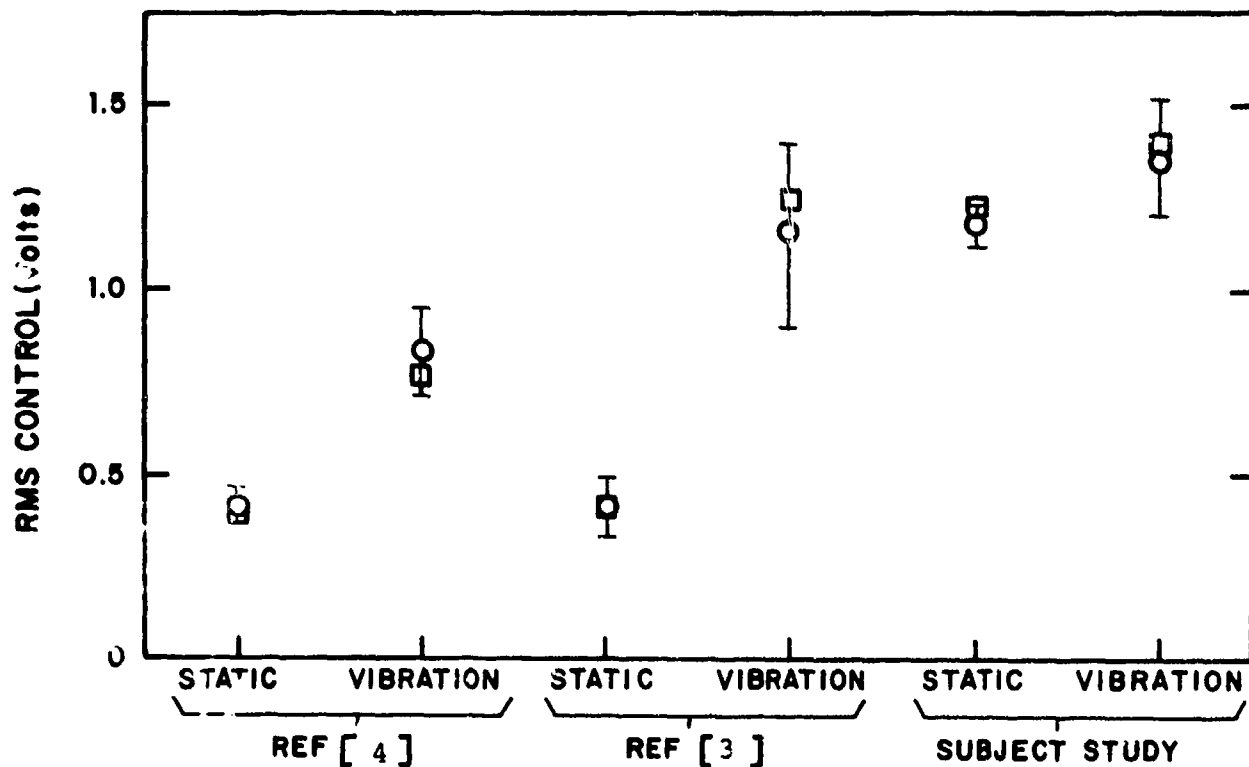
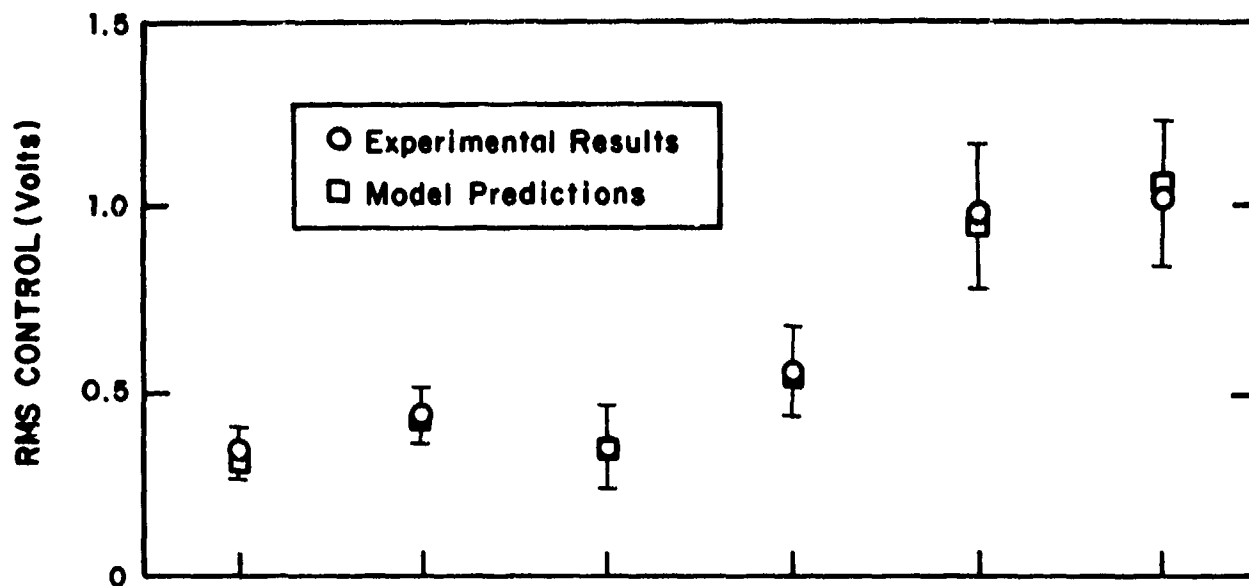
Stiff-Stick Configuration

Brackets indicate plus and minus one standard deviation about the experimental mean.

Experimental conditions represented in Figure 25 include the condition yielding maximal effects of vibration (X+pitch vibration) and as well as two conditions having intermediate effects (Z and roll vibration). Predicted error and control scores reproduced the trend of the experimental results quite well and in all cases were within one standard deviation of the experimental mean. Therefore, the relationship between pilot parameters and biodynamic response given in equation (5) would appear to be independent of the axis of platform vibration, at least for the pitch-axis tracking task.

Figure 26 compares predicted and experimental performance scores for three experimental studies of Z-axis vibration, using the same set of model parameters. Again, model results follow the trend of the experimental data and are within one standard deviation of the experimental mean. Since the experimental conditions explored in the three studies employed different control gains and different tracking amplitudes, these results provide a good test of the relationships shown in equation (5) relating pilot parameters to control force.

Predicted and measured frequency-response measures are compared in Figure 27. Static and X+pitch results are shown in Figure 27a for the pitch tracking task; Figure 27b compares measures obtained in the static environment (roll tracking task) with measures obtained in the roll-axis vibration environment for both pitch and roll tracking tasks. The model results reproduce the following effects of vibration found in the experimental data: (1) amplitude ratio at the highest measurement frequency increases



WHL-372

VIBRATION ENVIRONMENT

Figure 26. Comparison of Predicted and Measured Rms Performance Scores for Three Study Programs
Pitch-axis tracking, Z-axis vibration, stiff-stick configuration

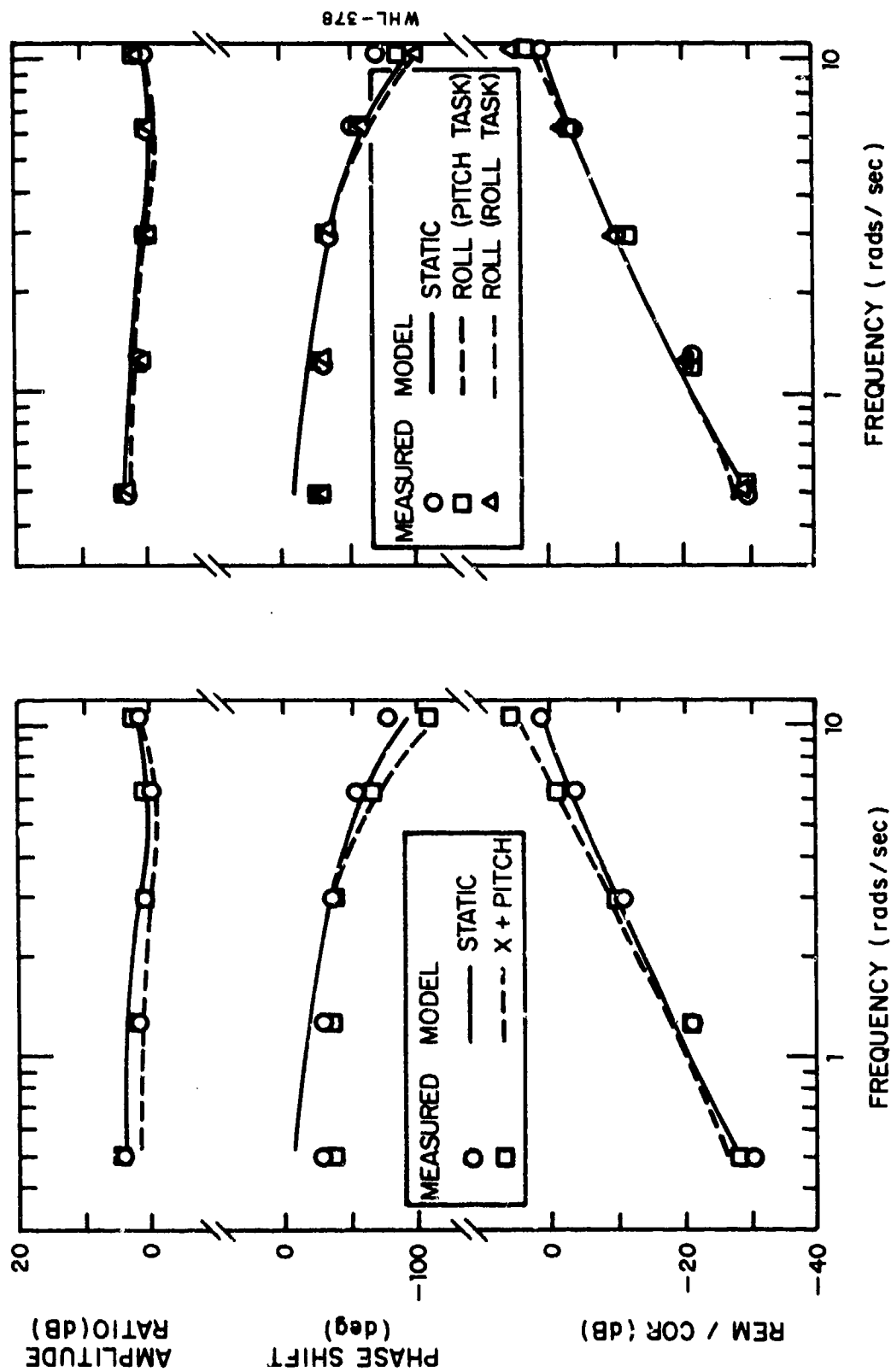


Figure 27. Comparison of Predicted and Measured Frequency Response

relative to amplitude ratio measurements at lower frequencies; (2) high-frequency phase lag increases; the ratio of remnant-related to input correlated power increases, especially at the highest measurement frequencies.

The model does not match all of the details of the measured response, however. The model predicts the same response behavior for both pitch-axis and roll-axis tracking behavior when the pilot is subjected to roll-axis platform vibration even though experimental results show a (statistically significant) greater performance degradation for the roll-axis tracking task.* This result suggests that the interface model of equation (5) might yield more accurate predictions if the directional aspects of shoulder and/or limb vibration are considered. Further study is required to determine whether or not directional effects are important.

Another difference between model and experimental results -- one that has been found consistently in previous studies as well [3,4] -- is that the predicted amplitude ratio is lower than the measured ratio under vibration conditions. Manipulation of the pilot-related model parameters, using the formulation of the pilot model described in the literature [6,7], does not allow us to match this aspect of pilot response behavior and simultaneously match other performance measures. Preliminary investigation with revised model formulations has indicated, however, that the pilot's amplitude response to vibration can be better matched, without sacrificing model matching along other dimensions, if we assume that the pilot does not have the correct perception

*Stick feedthrough, which depends strongly on the relation between the direction of vibration and the direction of control response, influences error and control scores but is assumed to have no appreciable effect on tracking *strategy*.

of the system control gain.* Specifically, if we allow the (mathematical) pilot to assume that the control gain is, say 1-2 dB lower than actual, the predicted pilot gain will be correspondingly increased. These results suggest that the presence of vibration impedes the pilot's ability to identify the control system. Further study is needed to determine whether or not a consistent rule for adjusting the pilot's estimate of control gain can be found to match the data obtained over the recent series of experiments.

The interface model of equation (5) was applied to selected spring-stick experiments, but it did not provide an adequate match to experimental results. In particular, the inverse relation between model parameters and control force seemed to be inappropriate. Accordingly, subsequent investigations were made with a revised interface model in which parameters varied inversely with predicted control *displacement*. Contract resources were not sufficient to test this revised model thoroughly, but preliminary results were encouraging.

*A modified version of the optimal-control pilot/vehicle model has been developed and implemented to allow the pilot to have an incorrect "internal model" of the control system [12].

4. SUMMARY AND RECOMMENDATIONS

A series of experiments was performed to explore biodynamic response and tracking performance in various whole-body vibration environments. The primary experimental variable was the direction of the vibration: X+pitch, Y+roll, Z, roll, pitch, and yaw. Tracking axis (pitch or roll) and control-stick spring constant were additional experimental variables. Data from these experiments were analyzed to derive engineering descriptions of biodynamic response and tracking behavior, and a model was developed to relate tracking performance to biodynamic response parameters.

The principal results of this study may be summarized as follows:

Effects of Vibration Axis. Vibration inputs causing front-back body motion (X+pitch, pitch) produced the greatest total rms shoulder acceleration, the greatest amount of stick feedthrough, and the greatest increase in tracking error. Z-axis vibration had a smaller effect; Y+roll, roll, and yaw vibrations had still smaller effects.

Stick Feedthrough. Stick feedthrough was represented in terms of the impedance model developed in earlier studies. The transfer impedance was relatively flat with frequency for situations involving longitudinal-axis vibration and control response, whereas transfer impedances involving lateral-axis vibration and control were U-shaped over the region of frequency investigated (2-10 Hz). Output impedances increased

asymptotically with frequency at 40 dB/decade for situations involving pitch-axis tracking, whereas the asymptotic increase was closer to 20 dB/decade for roll-axis tasks.

Biodynamic Cross-Coupling. Substantial cross-coupling was observed for Y, Z, and roll vibration inputs. Greatest linear coupling appeared to be in the axis of direct coupling.

Effects of Stick Parameters. As in earlier studies, stick spring constant had a substantial effect on tracking performance and stick feedthrough. Feedthrough, as well as vibration/static performance differences, were greater for the stiff-stick configuration, although tracking was better overall for this configuration. For all but Z-axis vibration, changes in stick configuration introduced a statistically significant change in rms shoulder acceleration.

Effects of Vibration on Tracking. Vibration generally caused a statistically significant increase in tracking error (relative to the static condition) for the stiff-stick experiments, whereas error was not significantly affected in the spring-stick experiments. In general, rms control scores were significantly increased by vibration for both control stick configurations. Vibration caused changes in pilot response behavior similar to those observed previously: (a) pilot gain was reduced at low frequencies and increased at the highest measurement frequency; (b) high-frequency phase shift increased; and (c) the spectrum of the pilot's

"remnant", relative to input-correlated power, increased. The changes were greater when the direction of vibration was along the axis of control.

Modeling. As in previous studies, the effects of vibration on tracking performance were modeled largely by increases in pilot time delay and motor noise. The submodel relating model parameters to biodynamic response, developed in the previous study, was modified to allow time delay and motor noise variance to vary linearly with rms shoulder acceleration and inversely with control force. A single set of model parameters provided a good match to stiff-stick results obtained in a number of experimental studies.

Despite the improved modeling capability developed in this study, certain inconsistencies in the vibration/tracking data remain and warrant further investigation. Feedthrough impedance functions computed for Z-axis vibration have not been consistent for the three most recent studies (including this one) conducted as part of the AMRL long-range program. Differing subject populations and control force requirements for the different studies were suggested earlier as possible causes of these discrepancies.

A consistent treatment of visual effects is also lacking. In the study of Levison and Houck [3], visual sources of vibration-related performance degradation were inferred, although they were of secondary importance compared to changes in time delay and motor-related interference. In the succeeding study [4], results were best modeled by the assumption of no visual-related interference.

In order to resolve these discrepancies, we suggest that an experimental program be conducted to explore, in a systematic fashion with a single set of subjects, variations in control gain, display gain, and tracking input. Such a study should provide definitive data for determining the importance of visual effects and for determining the source of differences in feed-through characteristics. Data would also be provided for a further test of the vibration/tracking interface submodel developed in this study, both for spring-stick as well as stiff-stick configurations.

Analysis of tracking performance in vibration has consistently shown that measured changes in pilot gain are less than those predicted by the model when a best overall match to pilot performance is achieved. As noted earlier, preliminary exploration with an advanced pilot model indicates that an improved match can be obtained if we assume that the pilot underestimates the control gain when subjected to vibration. Accordingly, we recommend that an analytical study be undertaken to determine whether or not the data obtained from recent studies as well as the subject study can be modeled in this manner, and, if so, to find a consistent rule for predicting the pilot's estimate of the control gain. No new experimental data would be required for this effort.

APPENDIX
SUPPLEMENTARY DATA

Table A1
Average RMS Biodynamic Response Acceleration

VIBRATION CONDITION	RMS Acceleration, g			
	Shoulder-X	Shoulder-Y	Shoulder-Z	Elbow

(a) PITCH TASK, STIFF STICK

X	0.69	0.34	0.17	0.28
Y	0.13	0.15	0.081	0.42
Z	0.22	0.26	0.26	0.41
ROLL	0.16	0.18	0.081	0.34
PITCH	0.64	0.29	0.15	0.27
YAW	0.085	0.059	0.030	0.15

(b) PITCH TASK, SPRING STICK

X	0.55	0.26	0.16	0.32
Y	0.11	0.12	0.069	0.36
Z	0.22	0.28	0.26	0.36
ROLL	0.15	0.15	0.071	0.38
PITCH	0.52	0.23	0.13	0.28
YAW	0.081	0.049	0.024	0.14

(c) ROLL TASK, STIFF STICK

Y	0.12	0.15	0.089	0.46
ROLL	0.16	0.18	0.087	0.37
YAW	0.088	0.057	0.032	0.17

(d) ROLL TASK, SPRING STICK

Y	0.11	0.14	0.073	0.43
ROLL	0.14	0.16	0.081	0.43
YAW	0.078	0.051	0.026	0.16

Table A2
Average Control/Platform Describing Functions

VIBRATION CONDITION	AMPLITUDE RATIO (dB)					PHASE SHIFT (deg)				
	FREQUENCY (rad/sec)					FREQUENCY (rad/sec)				
	12.4	20.8	31.4	44.1	63.3	12.4	20.8	31.4	44.1	63.3

(a) PITCH TASK, STIFF STICK

X	15.3	14.2	15.5	13.4	14.8	-21	-6	-21	-26	-60
Y	9.7	1.0	-1.6	-0.1	2.9	136	88	130	124	104
Z	-3.5	0.5	-1.1	-0.9	5.6	198	185	146	187	106
ROLL	-11.4	-18.1	-21.0	-20.7	-20.6	132	98	99	94	77
PITCH	-6.5	-6.0	-5.4	-8.3	-9.2	0	-9	-37	-48	-72
YAW	-12.6	-16.9	-16.5	-16.6	-17.0	-8	-27	-21	-19	-28

(b) PITCH TASK, SPRING STICK

X	9.2	9.6	6.3	-3.5	-8.2	-52	-66	-140	-154	-192
Y	-7.5	-7.8	-17.8	-24.6	-32.9	139	45	-23	-128	-178
Z	-5.9	-7.2	-16.5	-19.2	-27.8	-80	-207	-325	-282	-320
ROLL	-25.9	-27.5	-34.0	-41.9	-50.3	86	52	-25	-89	-157
PITCH	-13.9	-9.6	-15.0	-25.4	-31.7	-19	-67	-154	-179	-204
YAW	-20.3	-21.8	-26.0	-34.4	-41.0	-62	-74	-141	-149	-153

(c) ROLL TASK, STIFF STICK

Y	17.7	3.9	3.3	6.2	10.8	-40	-100	1	-10	-8
ROLL	-4.8	-15.4	-21.0	-17.5	-13.2	-44	-83	-33	-19	-21
YAW	-11.6	-18.4	-29.3	-29.7	-26.6	163	63	-50	-172	101

(d) ROLL TASK, SPRING STICK

Y	7.5	2.6	2.5	-1.2	-2.9	-72	-80	-106	-133	-153
ROLL	-14.9	-17.3	-20.2	-24.2	-27.1	-77	-88	-125	-143	-164
YAW	-20.2	-23.4	-27.0	-44.5	-50.8	107	-5	-166	-231	-401

0 dB = 1 volt/g for translational vibration.

0 dB = 1 volt/(rad/sec²) for rotational vibration.

Table A3
Impedance Model for Stick Feedthrough

VIBRATION CONDITION	AMPLITUDE RATIO (dB) FREQUENCY (rad/sec)					PHASE SHIFT (deg) FREQUENCY (rad/sec)				
	12.4	20.8	31.4	44.1	63.3	12.4	20.8	31.4	44.1	63.3

(a) TRANSFER IMPEDANCE, PITCH TASK

X	16.0	14.8	15.7	13.0	13.5	-20	-4	-18	-20	-50
Y	11.6	1.9	-2.2	-1.0	-0.1	135	90	133	107	43
Z	-3.1	1.3	-1.1	-1.1	0.4	196	187	152	195	127
ROLL	-10.3	-17.3	-21.0	-22.2	-23.6	137	101	103	93	55
PITCH	-5.6	-5.4	-5.3	-8.8	-10.4	1	-8	-34	-42	-63
YAW	-11.9	-16.2	-16.3	-17.1	-18.3	-5	-26	-19	-13	-15

(b) OUTPUT IMPEDANCE, PITCH TASK

X	10.5	14.5	20.5	25.4	29.3	129	139	149	144	144
Y	23.9	13.8	25.9	32.3	40.9	-7	101	165	232	221
Z	17.4	10.1	24.6	26.5	36.1	211	103	134	128	164
ROLL	21.4	14.8	23.2	28.9	34.8	77	99	150	184	214
PITCH	6.1	14.1	20.6	25.5	28.9	108	145	147	147	144
YAW	15.7	12.5	20.7	26.2	30.3	121	136	149	146	139

(c) TRANSFER IMPEDANCE, ROLL TASK

Y	18.7	4.5	3.7	6.4	10.5	-38	-101	2	-80	-5
ROLL	-3.8	-14.7	-20.5	-17.3	-13.5	-42	-83	-32	-18	-18
YAW	-10.9	-17.4	-28.9	-28.8	-28.4	165	65	-49	-166	-250

(d) OUTPUT IMPEDANCE, ROLL TASK

Y	13.7	11.3	16.1	17.9	20.6	81	207	163	152	154
ROLL	14.6	9.1	14.9	17.5	20.7	83	184	164	153	153
YAW	16.3	15.5	15.8	22.3	30.1	117	140	171	77	154

0 dB = 1 pound/g for transfer impedance for translational platform vibration.

0 dB = 1 pound/(rad/sec²) for transfer impedance for rotational platform vibration.

0 dB = 1 pound/inch for output impedance.

Table A4
Average Shoulder-X/Platform Describing
Functions

VIBRATION CONDITION	AMPLITUDE RATIO (dB)					PHASE SHIFT (deg)				
	FREQUENCY (rad/sec)					FREQUENCY (rad/sec)				
	12.4	20.8	31.4	44.1	63.3	12.4	20.8	31.4	44.1	63.3

(a) PITCH TASK, STIFF STICK

X	2.5	4.6	5.9	4.7	-0.1	-13	-27	-61	-98	-168
Y	-4.4	-3.9	-5.8	-10.0	-31.7	214	157	117	78	93
Z	-12.9	-14.9	-11.6	-4.0	-5.1	167	127	21	-114	-189
ROLL	-23.3	-23.9	-26.5	-31.6	-41.2	196	145	102	68	107
PITCH	-14.9	-13.6	-11.8	-16.1	-21.8	-15	-32	-72	-118	-173
YAW	-29.0	-24.8	-24.7	-29.2	-36.5	10	-15	-62	-93	-126

(b) PITCH TASK, SPRING STICK

X	3.4	5.4	2.8	1.0	2.8	-14	-41	-63	-76	-149
Y	-6.0	-7.1	-10.2	-15.2	-9.9	194	145	121	91	84
Z	-25.8	-14.0	-5.5	-2.6	-9.1	136	67	20	-77	-142
ROLL	-24.3	-26.1	-28.9	-30.7	-32.5	181	139	115	82	58
PITCH	-14.5	-12.8	-15.9	-18.3	-18.7	-16	-47	-72	-95	-153
YAW	-27.8	-24.3	-28.8	-36.4	-34.1	3	-35	-90	-74	-101

(c) ROLL TASK, STIFF STICK

Y	-4.3	-5.9	-6.6	-8.3	-12.4	196	155	129	97	2
ROLL	-24.1	-25.4	-26.3	-28.0	-40.8	190	151	126	76	30
YAW	-28.2	-26.3	-24.9	-28.7	-33.3	1	-11	-51	-77	-132

(d) ROLL TASK, SPRING STICK

Y	-4.7	-5.7	-8.6	-12.6	-11.3	200	145	117	85	84
ROLL	-24.2	-25.2	-28.3	-31.7	-32.7	190	139	111	86	57
YAW	-28.1	-25.2	-25.6	-34.0	-36.9	2	-25	-69	-103	-125

0 dB = 1g/g for translational vibration.

0 dB = 1g/(rad/sec²) for rotational vibration.

Table A5
Average Shoulder-V/Platform Describing
Functions

VIBRATION CONL TION	AMPLITUDE RATIO (dB)					PHASE SHIFT (deg)				
	FREQUENCY (rad/sec)					FREQUENCY (rad/sec)				
	12.4	20.8	31.4	44.1	63.3	12.4	20.8	31.4	44.1	63.3

(a) PITCH TASK, STIFF STICK

X	-9.4	-8.2	-2.8	1.0	0.1	-27	-34	-68	-106	-192
Y	1.0	-6.2	-16.1	-10.5	-9.8	-76	-144	15	-43	-101
Z	-8.4	-6.2	-3.3	-7.4	-3.7	-5	1	-26	-84	-65
ROLL	-19.1	-28.9	-30.7	-27.6	-28.0	-73	-98	-41	-50	-99
PITCH	-26.7	-24.7	-19.8	-20.2	-22.4	-18	-35	-69	-128	-184
YAW	-29.9	-34.1	-37.9	-35.9	-35.7	141	67	-73	-164	-218

(b) PITCH TASK, SPRING STICK

X	-13.7	-13.1	-4.2	-2.4	-0.4	-15	-26	-42	-94	-180
Y	-0.4	-8.5	-20.9	-22.1	-16.7	-93	-145	-116	-96	-84
Z	-5.6	-3.0	-1.4	-5.6	-11.1	-11	-20	-62	-135	-69
ROLL	-19.8	-30.3	-33.2	-33.3	-30.6	-87	-109	-71	-54	-88
PITCH	-28.8	-27.9	-23.7	-22.4	-22.8	-16	-51	-55	109	-179
YAW	-29.8	-32.4	-43.2	-45.0	-45.0	129	56	-62	3	-167

(c) ROLL TASK, STIFF STICK

Y	1.4	-5.4	-21.7	-12.1	-8.4	-69	-137	-32	-60	-103
ROLL	-18.9	-28.9	-31.0	-28.2	-27.3	-69	-93	-49	-49	-87
YAW	-30.3	-30.5	-43.2	-39.7	-38.9	153	82	-43	-171	-223

(d) ROLL TASK, SPRING STICK

Y	0.7	-7.0	-23.1	-14.1	-16.1	-83	-148	-29	-66	-89
ROLL	-19.3	-29.9	-31.7	-30.1	-29.1	-78	-99	-57	-52	-82
YAW	-30.7	-30.9	-39.3	-39.7	-40.9	141	76	-46	-197	-210

0 dB = 1 g/g for translational vibration.

0 dB = 1 g/(rad/sec²) for rotational vibration.

Table A6

Average Shoulder-Z/Platform Describing
Functions

VIBRATION CONDITION	AMPLITUDE RATIO (dB) FREQUENCY (rad/sec)					PHASE SHIFT (deg) FREQUENCY (rad/sec)				
	12.4	20.8	31.4	44.1	63.3	12.4	20.8	31.4	44.1	63.3

(a) PITCH TASK, STIFF STICK

X	-25.3	-14.1	-7.0	-6.7	-6.5	91	98	20	-41	-122
Y	-8.0	-8.8	-12.9	-15.5	-17.5	106	32	-20	-61	-97
Z	-1.3	0.5	1.0	0.5	-2.6	-2	-9	-28	-59	-77
ROLL	-29.1	-28.8	-32.8	-35.1	-35.8	80	16	-20	-32	-50
PITCH	-36.1	-33.8	-25.6	-26.0	-26.5	10	30	-4	-55	-116
YAW	-40.1	-37.6	-39.0	-38.9	-56.3	-34	-95	-151	-196	-268

(b) PITCH TASK, SPRING STICK

X	-13.9	-6.6	-5.0	-10.9	-10.1	152	116	33	-17	-99
Y	-8.9	-9.2	-13.8	-23.3	-35.9	119	42	-33	-19	-140
Z	-1.3	1.0	1.1	-0.9	-6.0	-2	-15	-47	-74	-96
ROLL	-29.9	-31.0	-36.5	-43.3	-40.9	88	14	-33	-24	-27
PITCH	-42.0	-31.1	-26.4	-27.6	-29.7	115	96	20	-36	-108
YAW	-39.7	-39.8	-42.8	-42.7	-49.0	-25	-84	-131	-238	-403

(c) ROLL TASK, STIFF STICK

Y	-7.1	-7.9	-11.4	-13.7	-12.9	105	38	-10	-40	-85
ROLL	-27.7	-28.8	-32.2	-32.6	-32.8	83	19	-4	-20	-50
YAW	-39.4	-35.4	-38.4	-38.7	-47.6	-27	-96	-152	-186	-215

(d) ROLL TASK, SPRING STICK

Y	-6.4	-8.4	-12.7	-17.7	-29.1	103	33	-23	-72	-62
ROLL	-27.1	-28.9	-34.2	-38.1	-37.4	84	16	-19	-21	-33
YAW	-39.2	-36.3	-39.4	-39.2	-54.7	-28	-96	-158	-218	-333

0 dB = g/g for translational vibration.

0 dB = 1 g/(rad/sec²) for rotational vibration.

Table A7

Average Elbow/Platform Describing Functions

VIBRATION CONDITION	AMPLITUDE RATIO (dB)					PHASE SHIFT (deg)				
	FREQUENCY (rad/sec)					FREQUENCY (rad/sec)				
	12.4	20.8	31.4	44.1	63.3	12.4	20.8	31.4	44.1	63.3

(a) PITCH TASK, STIFF STICK

X	-12.6	-18.8	-8.3	-0.5	-2.3	-22	59	29	-71	-229
Y	2.9	-0.6	0.3	4.0	7.1	-54	-68	-55	-78	-118
Z	-16.8	-9.8	-5.2	2.6	-3.1	-6	-51	-89	-173	-207
ROLL	-18.9	-21.9	-22.6	-20.7	-17.2	-67	-78	-82	-96	-132
PITCH	-31.2	-33.3	-29.5	-22.1	-22.0	-9	-40	-8	-117	-240
YAW	-32.5	-31.9	-43.4	-28.5	-25.3	139	89	-125	-216	-302

(b) PITCH TASK, SPRING STICK

X	-16.0	-10.6	-2.5	-3.4	-3.0	-26	53	-49	-125	-247
Y	5.5	2.3	0.5	3.6	5.4	-60	-106	-102	-136	-199
Z	-17.8	-14.5	-9.9	-2.5	-3.1	-111	-127	-128	-203	-234
ROLL	-16.0	-19.8	-21.1	-19.9	-18.9	-70	-116	-128	-161	-216
PITCH	-34.9	-33.4	-30.2	-25.5	-23.6	1	-38	-61	-140	-267
YAW	-31.8	-28.8	-32.7	-32.6	-32.2	127	58	-65	-240	-342

(c) ROLL TASK, STIFF STICK

Y	3.6	-1.9	0.9	5.5	7.5	-52	-75	-41	-78	-108
ROLL	-17.7	-22.6	-23.5	-19.8	-16.7	-61	-82	-66	-83	-122
YAW	-34.3	-31.3	-40.9	-29.0	-26.3	156	81	-113	-216	-304

(d) ROLL TASK, SPRING STICK

Y	5.8	2.1	4.5	5.7	7.2	-65	-88	-100	-132	-173
ROLL	-16.1	-18.8	-19.1	-18.5	-17.1	-78	-104	-129	-158	-204
YAW	-29.2	-28	-39.2	-30.3	-30.8	123	43	-160	-252	-332

0 dB = 1 g/g for translational vibration.

0 dB = 1 g/(rad/sec²) for rotational vibration.

Table A8
Average RMS Tracking Scores

VIBRATION CONDITION	RMS Score, Volts			
	STIFF ERROR	STICK CONTROL	SPRING ERROR	STICK CONTROL

(a) PITCH TASK

STATIC	0.98	1.18	1.20	1.25
X	1.17	2.18	1.23	1.49
Y	0.98	1.42	1.22	1.32
Z	1.04	1.36	1.24	1.25
ROLL	1.02	1.40	1.20	1.34
PITCH	1.15	1.95	1.22	1.42
YAW	1.04	1.27	1.22	1.25

(b) ROLL TASK

STATIC	1.04	1.17	1.26	1.18
Y	1.14	1.58	1.34	1.34
ROLL	1.16	1.59	1.36	1.36
YAW	1.14	1.30	1.35	1.21

Table A9
Average Frequency-Response Measures, Stiff Stick

VIBRATION CONDITION	AMPLITUDE RATIO (dB) FREQUENCY (rad/sec)					PHASE SHIFT (deg) FREQUENCY (rad/sec)					REM/COR (dB) FREQUENCY (rad/sec)				
	0.5	1.25	3.0	6.3	10.5	0.5	1.25	3.0	6.3	10.5	0.5	1.25	3.0	6.3	10.5
(a) PITCH TASK															
STATIC	4.0	2.4	1.3	0.6	1.8	-29	-29	-37	-55	-78	-31.4	-22.7	-12.7	-4.3	0.7
X	4.6	2.3	1.3	1.7	3.3	-36	-35	-39	-64	-108	-28.3	-21.2	-9.6	-0.8	5.9
Y	4.6	2.6	1.7	2.1	3.5	-29	-29	-35	-58	-88	-31.8	-22.8	-12.4	-4.2	2.8
Z	3.7	1.7	0.7	1.0	2.5	-26	-27	-36	-58	-93	-33.2	-22.2	-12.0	-3.9	2.5
ROLL	3.5	2.0	1.1	1.4	3.1	-25	-27	-34	-56	-88	-29.8	-21.6	-12.0	-2.5	3.8
PITCH	4.0	2.2	1.2	1.4	2.9	-32	-31	-40	-63	-103	-29.8	-20.1	-9.4	-2.1	5.6
YAW	3.2	1.6	0.6	0.4	1.7	-26	-27	-37	-59	-88	-30.1	-21.5	-11.6	-3.4	1.7
(b) ROLL TASK															
STATIC	3.9	1.7	0.6	0.2	1.0	-30	-31	-36	-52	-71	-29.9	-21.7	-10.5	-3.4	1.3
Y	3.8	1.6	0.3	1.0	2.2	-32	-34	-39	-62	-98	-30.6	-21.9	-10.2	-2.0	5.4
ROLL	3.2	1.1	0.0	1.0	2.6	-32	-30	-36	-58	-97	-30.0	-19.6	-10.0	-1.7	5.9
YAW	3.2	1.0	0.2	0.2	1.2	-32	-32	-36	-60	-91	-29.8	-18.0	-8.4	-1.5	3.8

Table A10
Average Frequency-Response Measures, Spring Stick

VIBRATION CONDITION	AMPLITUDE RATIO (dB) FREQUENCY (rad/sec)					PHASE SHIFT (deg) FREQUENCY (rad/sec)					REM/COR (dB) FREQUENCY (rad/sec)				
	0.5	1.25	3.0	6.3	10.5	0.5	1.25	3.0	6.3	10.5	0.5	1.25	3.0	6.3	10.5
(a) PITCH TASK															
STATIC	1.8	0.8	0.0	-1.1	0.6	-23	-23	-43	-67	-97	-29.9	-20.4	-9.7	-1.6	2.4
X	2.8	1.4	0.0	-0.4	1.8	-24	-27	-45	-72	-109	-30.7	-22.2	-10.5	-1.9	5.0
Y	2.2	0.9	0.1	-0.5	1.4	-26	-24	-44	-71	-104	-29.6	-22.3	-10.8	-2.4	2.8
Z	1.3	0.2	-0.6	-1.1	1.3	-25	-24	-42	-69	-106	-29.6	-20.6	-9.7	-2.0	2.4
ROLL	2.3	1.2	0.2	-0.1	2.2	-25	-25	-42	-71	-105	-31.9	-20.4	-9.7	-2.0	2.6
PITCH	2.4	1.0	-0.2	-0.5	1.7	-23	-25	-44	-72	-115	-29.6	-22.1	-10.3	-1.4	4.2
YAW	1.8	0.5	-0.3	-1.3	0.7	-24	-23	-43	-70	-103	-30.9	-21.8	-10.0	-2.4	2.4
(b) ROLL TASK															
STATIC	0.6	-0.5	-1.3	-1.6	-0.2	-30	-16	-40	-67	-93	-30.3	-20.5	-9.4	-1.9	2.7
Y	0.9	-0.4	-0.9	-0.6	1.5	-23	-22	-43	-72	-118	-28.4	-19.9	-9.3	-1.2	4.4
ROLL	0.5	-0.8	-1.3	-0.7	1.2	-22	-21	-41	-74	-127	-28.3	-19.3	-8.3	-1.2	5.6
YAW	0.2	-1.0	-1.9	-1.8	-0.3	-20	-17	-42	-72	-113	-30.2	-19.4	-7.4	-1.2	5.4

Table A11

Significance of Vibration/Static Differences in Frequency Response, Stiff Stick

VIBRATION CONDITION	AMPLITUDE RATIO (dB) FREQUENCY (rad/sec)					PHASE SHIFT (deg) FREQUENCY (rad/sec)					REM / COR (dB) FREQUENCY (rad/sec)				
	0.5	1.25	3.0	6.3	10.5	0.5	1.25	3.0	6.3	10.5	0.5	1.25	3.0	6.3	10.5
(a) PITCH TASK															
X+PITCH	-	-	-	.05	.01	.1	.01	-	.01	.001	-	-	.01	.01	.001
Y+ROLL	-	-	-	.01	.001	-	-	-	-	.01	-	-	-	-	.01
Z	-	-	.05	-	.05	-	-	-	-	.001	-	-	-	-	.01
ROLL	-	-	-	.05	.01	-	-	-	-	.001	-	-	-	.05	.001
PITCH	-	-	-	-	.05	-	-	.05	.001	.001	-	-	.05	.05	.001
YAW	-	-	-	-	-	-	-	-	.01	.001	-	-	-	-	-
(b) ROLL TASK															
Y+ROLL	-	-	-	-	.05	-	-	-	.01	.001	-	-	-	-	.01
ROLL	-	-	-	-	.01	-	-	-	.01	.001	-	-	-	.05	.001
YAW	-	-	-	-	-	-	-	-	.05	.001	-	.05	-	-	.01

Entries indicate level of significance.

Table A12

Significance of Vibration/Static Differences in Frequency Response, Spring Stick

VIBRATION CONDITION	AMPLITUDE RATIO (dB) FREQUENCY (rad/sec)					PHASE SHIFT (deg) FREQUENCY (rad/sec)					REM / COR (dB) FREQUENCY (rad/sec)				
	0.5	1.25	3.0	6.3	10.5	0.5	1.25	3.0	6.3	10.5	0.5	1.25	3.0	6.3	10.5
(a) PITCH TASK															
X+PITCH	.05	-	-	.05	.05	-	-	.05	.01	.001	-	-	-	-	.01
Y+ROLL	-	-	-	-	-	-	-	-	.05	.01	-	.05	-	-	-
Z	-	.05	.01	-	.01	.05	-	-	.05	.001	-	-	-	-	-
ROLL	-	-	-	-	.05	-	-	-	.05	.001	-	-	-	-	-
PITCH	-	-	-	-	.05	-	-	-	.01	.001	-	-	-	-	.05
YAW	-	-	-	-	-	-	-	-	-	.05	-	-	-	-	-
(b) ROLL TASK															
Y+ROLL	-	-	-	-	-	-	.01	-	.05	.001	-	-	-	-	-
ROLL	-	-	-	-	-	-	.001	-	.01	.001	-	-	-	-	.05
YAW	-	-	-	-	-	-	-	-	.01	.001	-	-	-	-	.05

Entries indicate level of significance.

Table A13

Significance of Pitch-Task/Roll-Task Differences in Frequency Response

VIBRATION CONDITION	AMPLITUDE RATIO (dB) FREQUENCY (rad/sec)					PHASE SHIFT (deg) FREQUENCY (rad/sec)					REM/COR (dB) FREQUENCY (rad/sec)				
	0.5	1.25	3.0	6.3	10.5	0.5	1.25	3.0	6.3	10.5	0.5	1.25	3.0	6.3	10.5
(a) STIFF STICK															
STATIC	-	-	-	-	.05	-	-	-	-	-	-	-	-	-	-
Y-ROLL	-	.05	.001	.01	.01	-	.05	.05	-	.01	-	-	.01	.05	.01
ROLL	-	.05	.01	.05	.05	-	-	-	-	.01	-	.05	.01	-	.01
YAW	-	-	.05	-	-	-	-	-	-	.05	-	-	-	-	.01
(b) SPRING STICK															
STATIC	-	-	-	-	-	-	-	-	-	-	-	-	-	-	-
Y+ROLL	.05	.05	.05	-	-	-	-	-	-	.001	-	.001	-	-	.05
ROLL	.01	.001	.05	-	-	-	-	-	-	.001	.001	-	-	-	.001
YAW	.01	.05	.001	-	-	.05	.01	-	-	.01	-	-	-	-	.05

Entries indicate level of significance.

REFERENCES

1. Allen, R. W., Henry R. Jex and R. E. Magdaleno, Manual Control Performance and Dynamic Response During Sinusoidal Vibration, AMRL-TR-73-78, Aerospace Medical Research Laboratory, Wright-Patterson Air Force Base, Ohio, October 1973. [AD 773844]
2. Levison, William H., Analysis of Vibration-Induced Pilot Remnant, BBN Report No. 2608, Final Report, Bolt Beranek and Newman Inc., Cambridge, Mass., under Contract No. F33615-71-C-1207, August 1973.
3. Levison, William H. and Philip D. Houck, Guide for the Design of Control Sticks in Vibration Environments, AMRL-TR-74-127, Aerospace Medical Research Laboratory, Wright-Patterson Air Force Base, Ohio, February 1975. [AD A-008533]
4. Levison, William H., Biomechanical Response and Manual Tracking Performance in Sinusoidal, Sum-of-Sines, and Random Vibration Environments, Aerospace Medical Research Laboratory, Wright-Patterson Air Force Base, Ohio, April 1976.
5. Berliner, Jeffrey E., and William H. Levison, PIVIB: A Computer Program for Analysis of Pilot Biodynamic and Tracking Response to Vibration, AMRL-TR-77-72, Aerospace Medical Research Laboratory, Wright-Patterson Air Force Base, Ohio, September 1977.
6. Kleinman, D. L., S. Baron and W. H. Levison, "An Optimal-Control Model of Human Response, Part 1: Theory and Validation", Automatica, Vol. 6, pp. 357-369, 1970.
7. Kleinman, D. L., S. Baron and W. H. Levison, "A Control Theoretic Approach to Manned-Vehicle Systems Analysis", IEEE Trans. on Auto. Control, Vol. AC-16, No. 6, December 1971.
8. Kleinman, D. L. and S. Baron, Analytic Evaluation of Display Requirements for Approach to Landing, NASA CR-1952, November 1971.
9. Baron, S., and W. H. Levison, A Manual Control Theory Analysis of Vertical Situation Displays for STOL Aircraft, NASA CR-114620, April 1973.
10. Kleinman, D. L. and W. R. Killingsworth, A Predictive Pilot Model for STOL Aircraft Landing, NASA CR-2374, March 1974.

11. Baron, S. and W. H. Levison, "An Optimal Control Methodology for Analyzing the Effects of Display Parameters on Performance and Workload in Manual Flight Control", IEEE Transactions on Systems, Man, and Cybernetics, Vol. SMC-5, No. 4, July 1975.
12. Baron, S. and J. Berliner, MANMOD 1975: Human Internal Models and Scene-Perception Models, U. S. Army Missile Command, Redstone Arsenal, Alabama, Technical Report RC-CR-76-3, September 1975.